PANEL FLUTTER IN SUPERSONIC FLOW

Thesis by

Joe Griffin Eisley

In Partial Fulfillment of the Requirements

For the Degree of

Doctor of Philosophy

California Institute of Technology

Pasadena, California

1956

ACKNOWLEDGEMENTS

The author wishes to express his deep appreciation to Dr. Y. C. Fung for his help and encouragement in carrying out this research. His interest as well as that of Dr. E. E. Sechler were a constant source of inspiration.

He wishes also to express his thanks to Mrs. D. Eaton for carrying out the numerous calculations and to Mrs. E. Fox and Mrs. B. Wood for help in preparing the manuscript.

This study has been greatly aided by the Air Force which is sponsoring a research program in panel flutter at the Institute, and this aid is gratefully acknowledged.

ABSTRACT

The problem of panel flutter in a supersonic flow is treated in three parts. In the first the flutter of a simply supported rectangular plate is studied. Only small deflections are considered so that linear plate theory may be used. The flutter mode is described by a series expansion in terms of the normal modes of oscillation of the plate in a vacuum. Linearized aerodynamic theory is used. The exact aerodynamic solution as well as two simplifications--strip theory and quasi-steady theory--are discussed. Numerical calculations were made to determine flutter boundaries for plates of varying aspect ratio using strip theory aerodynamics for $M = 2$ and $M = \sqrt{2}$. The flutter mode was described by considering only two or three normal modes in the calculations.

The flutter of a two-dimensional buckled panel with clamped edges is studied both theoretically and experimentally. The flutter mode is described by a series expansion of functions which satisfy the boundary conditions for clamped edges. Quasi-steady linearized aerodynamics is used. Large deflections of the panel are considered. Numerical calculations have been made considering only the first two terms of the series expansion. The theoretical and experimental results are compared.

TABLE OF CONTENTS

LIST OF SYMBOLS

PART I

a	velocity of sound
h	plate thickness
k	reduced frequency
ℓ, m, m, r, s	integers
p	pressure
t	time
v	downwash velocity
x, y, z	coordinates
D	flexural rigidity of plate
E	Young's Modulus
L_1, L_2	plate dimensions
M	Mach number
Q	generalized force
T	kinetic energy
U	free stream velocity
V	potential energy
β	$\sqrt{M^2 - 1}$
γ	$\frac{2r\pi}{L_2\beta}$
η	$\eta_0 \cos\theta + z$
η_0	$\frac{x - \xi}{\beta}$
θ, ξ, η	variables of integration
μ	$(x - \xi)$
λ	$\frac{m\pi}{L_2\beta}$

μ	$\frac{\rho_a L_1}{\rho_s h}$
ρ_a	mass density of air
ρ_s	mass density of plate
σ	Ω/M
φ	velocity potential
φ_1	reduced potential
ψ	$\tan^{-1} \frac{ik}{m\pi}$
ω	circular frequency
Ω	$\frac{k M^2}{L_1 \beta^2}$
AR	aspect ratio

PART II

α	M^2-2/M^2-1
τ	$\frac{Ut}{L}$, dimensionless time
ξ	$\frac{x}{L}$, dimensionless coordinate
γ	$\sqrt{M^2-1}\ \frac{\rho_s h}{\rho_a L}$, mass ratio
Q	$\rho_a U^2 L^3 / D\pi^4 \sqrt{M^2-1}$, dynamic pressure ratio
H_o	first buckling load
λ_i	i^{th} component of initial arch
φ	phase relation
ν	Poisson's ratio

INTRODUCTION:

The problem of flutter of a thin elastic plate placed in a supersonic airstream is considered. This problem has been treated in two dimensions by Shen (Ref. 1), Miles (Ref. 2), Goland and Luke (Ref. 3), and Nelson and Cunningham (Ref. 4). A different problem, that of an infinitely long panel on equally spaced intermediate supports, has been treated by Hedgepeth, Budiansky, and Leonard (Ref. 5). Linear plate theory is used in the above.

The possibility of the flutter of a buckled panel also exists. This buckling may result from thermal expansion caused by aerodynamic heating or from other causes. This problem was first treated by considering the steady state stability of a buckled two-dimensional panel placed in a supersonic flow. Isaacs (Ref. 6), Hayes (Ref. 7), and Miles (Ref. 8) treated this problem but neglected the strain in the mid-surface of the plate caused by the membrane stress. Fung (Ref. 9) included this effect in treating the steady-state stability of a buckled panel. The non-steady or flutter problem of a two-dimensional buckled panel has been treated by Fung (Ref. 10). The effects of membrane stress have been included.

In Part I of this report linear plate theory is used to study the flutter of a single rectangular panel of finite aspect ratio placed in a supersonic flow. Since small deflections are assumed, linearized aerodynamics can be used over a large range of Mach numbers excluding the transonic region. The exact aerodynamic solution is complicated due to the boundary conditions involved so

further approximation is necessary for computational reasons. The simplest and most obvious is the strip theory approximation. It is used for the numerical calculations in Part I. Another possible approximation is the quasi-steady one. This method is outlined in Appendix A. No calculations have been made using it. The exact theory is carried out in some detail but no calculations have been made at this time.

It is further assumed that the flutter mode can be described by a series expansion in terms of the normal modes of oscillation in a vacuum. In the numerical calculations two and three normal modes are used to describe the flutter mode. The feasibility of this approach needs further discussion particularly in view of the fact that the basic equation of panel flutter is non-self-adjoint. This and the effects of other approximations are discussed later.

Many parameters affect the flutter boundaries of rectangular plates. Principal among these are plate boundary conditions, plate rigidity, mass density ratio of air and plate material, Mach number, plate aspect ratio, edge loading conditions and others. Only simply supported plates are considered in Part I. The other parameters mentioned above are varied over a range of values and calculations have been made showing their effect. The limiting case of zero plate rigidity, the membrane, is included. The results of the calculations have been plotted and the curves are presented at the end of this report. They are discussed in Part I.

In Part II the method used by Fung (Ref. 10) to treat the two-dimensional simply supported buckled panel is extended to the two-dimensional clamped panel. As in the above reference only small reduced frequencies are considered so that the quasi-steady simplification may be made. The flutter mode is represented by a series expansion of a set of functions which in themselves satisfy the boundary conditions. The functions chosen were first used by Iguchi (Ref. 11) for determining the buckling load of a clamped rectangular plate. Additional information is presented in Ref. 12. In the numerical work which follows only the first two of these functions were used. The effect of clamped edges rather than simply supported ones in general changes only the numerical results but does not change the nature of these results. Therefore the presentation given here is quite sketchy and discussion is kept to a minimum. For a more complete account of the method refer to Ref. 10.

In Part III an experimental program that was designed to determine the nature of the flutter of a two-dimensional buckled plate with clamped leading and trailing edges is described. Tests were conducted in the Caltech Jet Propulsion Laboratory 12-inch Supersonic Wind Tunnel. An aluminum plate was mounted on a flat plate model placed on the centerline of the tunnel working section. The model was designed so that the plate could be buckled from outside the tunnel by moving the plate trailing edge with respect to its leading edge. The principal parameters which could be varied are Mach number, tunnel static pressure, plate material

and thickness, and the amplitude of the buckle. Data were taken by recording the above parameters at the onset of flutter. Information as to the nature of the motion itself was taken by means of strain gages fastened to the surface of the plate. The signals from these gages were fed into a Miller recording oscillograph. In this way a time history of the motion was obtained.

Due to the short time available for the tests no attempt was made to determine the complete flutter boundaries for plates of this type. The main effort was to determine the nature of the motion in order to check with the assumptions and results of Part II and with other theoretical approaches. This is discussed further in the body of Part III.

PART I: THE FLUTTER OF SIMPLY SUPPORTED RECTANGULAR PLATES IN A SUPERSONIC FLOW

A. Aerodynamic Forces

The linearized potential equation for unsteady flow is

$$\beta^2 \frac{\partial^2 \varphi}{\partial x^2} - \frac{\partial^2 \varphi}{\partial y^2} - \frac{\partial^2 \varphi}{\partial z^2} + \frac{2M}{a} \frac{\partial^2 \varphi}{\partial x \partial t} + \frac{1}{a^2} \frac{\partial^2 \varphi}{\partial t^2} = 0 \qquad \text{(A-1)}$$

where $\beta^2 = M^2 - 1$; M is the Mach number; and a is the velocity of sound in the undisturbed stream. The flow is in the direction of the positive x axis. This equation has been solved in two dimensions by Miles (Ref. 13), Garrick and Rubinow (Ref. 14) and others; and by Garrick and Rubinow (Ref. 15) in three dimensions.

The particular problem to be solved is that of the pressure distribution on an oscillating simply supported rectangular plate placed in a supersonic airstream. It is assumed that the surface can be represented by a series expansion in terms of the normal modes of such a plate in a vacuum. Harmonic motion is assumed.

The exact solution to this problem is rather complicated; therefore an approximate solution based on strip theory is first carried out. The subsequent numerical calculations are based on this approach. The exact solution is then carried out in some detail. At this time no calculations have been made using this approach. Another approximate method in which the quasi-steady assumption is made has also been outlined. Since it is rather long and is not used for any numerical work it has been included as Appendix A.

a) Strip Theory

In the case of harmonic oscillations of the plate in a uniform two-dimensional flow with undisturbed speed U, the deflection surface, y, may be written as

$$\bar{y}(x,t) = y(x)\, e^{-i\omega t} \tag{A-2}$$

The downwash distribution, v, in the plane of the plate is

$$\bar{v}(x,t) = v(x)e^{-i\omega t} = \left\{ U \frac{\partial y(x)}{\partial x} - i\omega y(x) \right\} e^{-i\omega t} \tag{A-3}$$

The pressure distribution over the plate is (Ref. 13)

$$p(x,t) = \frac{\rho_a U^2}{\beta} e^{-i\omega t} \left\{ v(0)\, G(x) + \int_0^x G(x-\xi) \frac{\partial v}{\partial \xi} d\xi - \frac{i\omega}{U} \int_0^x G(x-\xi)\, v(\xi)\, d\xi \right\} \tag{A-4}$$

where ρ_a = the density of the undisturbed flow

M = Mach number

$v(0)$ = value of $v(x)$ at $x = 0$

$G(x)$ = $e^{i\Omega(x-\xi)} J_0(\sigma[x-\xi])$

Ω = $\frac{\kappa M^2}{L_1 \beta^2}$

σ = Ω / M

κ = $\omega L_1 / U$

J_0 = Bessel function of first kind.

The normal modes in a vacuum for a simply supported two dimension plate with edges at $x = 0, L_1$ are

$$y(x) = A_m \sin \frac{m\pi x}{L_1} \qquad (m = 1,2,\cdots) \tag{A-5}$$

The pressure distribution for the m^{th} mode has been worked out by Shen (Ref. 1). For convenience, let $L_1 = \pi$, then

$$p_m = A_m \frac{\rho_a U^2}{2\beta\pi^2} \sqrt{m^2\pi^2 - k^2}\, e^{-i(\omega t - \Omega x)} \left\{ 2\pi \cos\psi\, J_0(\sigma x) \right.$$

$$\left. - i(m\pi + k) e^{-i\psi} \Phi_A + i(m\pi - k) e^{i\psi} \Phi_B \right\} \tag{A-6}$$

Φ_A, Φ_B in the above equation are defined by the following integrals

$$\Phi_A = \int_0^x e^{-i(\Omega+m)\xi} J_0(\sigma\aleph)\, d\xi$$

$$= \frac{1}{\sigma} e^{-i(\Omega+m)x} \int_0^{\sigma x} e^{i(\Omega+m)\aleph} J_0(\sigma\aleph)\, d(\sigma\aleph)$$

$$\Phi_B = \int_0^x e^{-i(\Omega-m)\xi} J_0(\sigma\aleph)\, d\xi \tag{A-7}$$

$$= \frac{1}{\sigma} e^{-i(\Omega-m)x} \int_0^{\sigma x} e^{i(\Omega-m)\aleph} J_0(\sigma\aleph)\, d(\sigma\aleph)$$

where $\aleph = x - \xi$

and $\psi = \tan^{-1} \frac{ik}{m\pi}$

These integrals can be reduced to a form

$$f_0(a,b) = \frac{1}{b} \int_0^b e^{-i\mu} J_0\left(\frac{\mu}{a}\right) d\mu \tag{A-8}$$

which is called the Schwarz function and is discussed in Ref. (16) and is tabulated in Refs. (14), (16), (17). Identities and asymptotic expansions are given in Ref. (1).

Specifically

$$\begin{aligned} \varphi_A &= x e^{-i(\Omega+m)x}\, \bar{f}_o\left[\frac{\Omega+m}{\sigma}, (\Omega+m)x\right] \\ &= x e^{-i(\Omega-m)x}\, \bar{f}_o\left[\frac{\Omega-m}{\sigma}, (\Omega-m)x\right] \end{aligned} \tag{A-9}$$

where $\bar{f}_o$ is the conjugate of f_o.

This result may be extended directly to the three-dimensional case if the strip theory assumption is made. The normal modes in a vacuum for a simply supported rectangular plate of finite aspect ratio are (Fig. 1)

$$y(x,z) = A_{mn} \sin\frac{m\pi x}{L_1} \sin\frac{n\pi z}{L_2} \tag{A-10}$$

Since strip theory assumed the flow over any narrow strip parallel to the flow is represented by the two-dimensional solution the pressure for the mn^{th} mode may be found by multiplying equation A-6 by $\sin\frac{n\pi z}{L_2}$ and replacing A_m by A_{mn}. The result is:

$$\begin{aligned} p_{mn} = A_{mn} \frac{\rho_a U^2}{2\beta\pi^2}\sqrt{m^2\pi^2 - k^2} \sin\frac{n\pi z}{L_2} \Big\{ 2\pi \cos\Psi J_o(\sigma x) \\ - i(m\pi + k) e^{i\Psi} \varphi_A + i(m\pi - k) e^{i\Psi} \varphi_B \Big\} e^{-i(\omega t - \Omega x)} \end{aligned} \tag{A-11}$$

b) Exact Aerodynamic Theory

The exact solution to equation A-1 for harmonic motion is (Ref. 15)

$$\Phi(x,+0,z,t) = -\frac{1}{2\pi\beta}\int_0^x\int_{\eta_1}^{\eta_2} v(\xi,\eta)e^{-i\omega t}\,\frac{\left[e^{i\omega\tau_1} + e^{i\omega\tau_2}\right]}{\sqrt{(\eta-\eta_1)(\eta_2-\eta)}}\,d\eta\,d\xi \qquad \text{(A-12)}$$

where

$$\tau_1 = \frac{M(x-\xi)}{a\beta^2} - \frac{\sqrt{(\eta-\eta_1)(\eta_2-\eta)}}{a\beta}$$

$$\tau_2 = \frac{M(x-\xi)}{a\beta^2} + \frac{\sqrt{(\eta-\eta_1)(\eta_2-\eta)}}{a\beta}$$

$$\eta_1 = z - \eta_0$$

$$\eta_2 = z + \eta_0$$

$$\eta_0 = \frac{(x-\xi)}{\beta}$$

The above integral represents an integration over the forward Mach cone. For points within the tip Mach cones (shaded area in Fig. 2) this area of integration includes a region off the plate itself. The boundary conditions on ϕ are

$$\frac{\partial\Phi}{\partial y} = \frac{\partial\gamma}{\partial t} + U\frac{\partial\gamma}{\partial x} \qquad \text{(A-31)}$$

on the surface of the plate and

$$\frac{\partial\Phi}{\partial y} = 0$$

in the regions $z < 0$, $z > L_2$

To integrate equation A-12 directly for a single rectangular panel of finite width is very difficult. A possible approach to overcome this difficulty is explained in the following:

An infinite plate in the direction perpendicular to the flow is considered. This plate is made up of an infinite number of bays of the dimensions given in Fig. 1. The front and rear edges are simply supported. The plate is continuous at the juncture of the bays and is free to rotate but may not deflect at this point. A deflection of the form

$$y_1 = A_{mn} \sin \frac{m\pi x}{L_1} \sin \frac{m\pi z}{L_2} \qquad \text{(A-14)}$$

is assumed. This corresponds to the normal modes of a rectangular simply supported plate as well as to the infinite plate just described. The first mode is illustrated in Fig. 3. The velocity potential and hence the pressure distribution may be found for this case from equation A-12 as will be shown shortly.

Now another infinite plate is considered. In it each bay is a separate simply supported plate. It is further assumed that all bays are oscillating in phase with one another. A deflection of the form

$$y_1 = A_{mn} \sin \frac{m\pi x}{L_1} \left\{ A_0 + \sum_{r=1}^{\infty} A_r \cos \frac{2\pi r z}{L_2} \right\}$$

is assumed.

$$A_0 = \frac{2}{m\pi}$$

$$A_r = \frac{1}{\pi\left(\frac{m}{2}+r\right)} \left\{ 1 - \cos\left(\frac{m}{2}+r\right)\pi \right\} \qquad \left(\frac{m}{2} = r\right) \qquad \text{(A-15)}$$

$$A_r = \frac{1}{\pi\left(\frac{m}{2}+r\right)}\left\{1-\cos\left(\frac{m}{2}+r\right)\pi\right\} + \frac{1}{\pi\left(\frac{m}{2}-r\right)}\left\{1-\cos\left(\frac{m}{2}-r\right)\pi\right\} \qquad \left(\frac{m}{2} \neq r\right)$$

This also corresponds to the normal modes of a single simply supported rectangular plate in a vacuum. The first mode for the infinite plate is illustrated in Fig. 4.

If the potentials obtained for these two cases are added, the potential is double for those bays oscillating in phase and is cancelled for those out of phase. Thus if the aspect ratio is large enough so the area of integration of equation A-12 extends only into the adjacent bays then the conditions of equation A-13 are satisfied if the resulting potential is divided by 2.

In the following only the case with the deflection according to equation A-14 will be carried out. This is not without value in itself since an infinite plate of this type is also an interesting problem. The strip theory solution for this infinite plate problem is identical to the single panel strip theory solution since the effect of adjacent panels is zero in the strip theory case.

Equation A-12 can be simplified by the following substitution

$$\eta = \eta_0 \cos\theta + z \tag{A-16}$$

The velocity potential is then

$$\varphi(x,+0,z,t) = -\frac{1}{2\pi\beta}\int_0^x\int_0^\pi v(\xi,\eta[\theta])\, e^{-i\omega t}\left[e^{i\omega\tau_1} + e^{i\omega\tau_2}\right] d\theta\, d\xi \tag{A-17}$$

where

$$\tau_1 = \frac{x-\xi}{a\beta^2}\left(M - \sin\theta\right)$$

$$\tau_2 = \frac{x-\xi}{a\beta^2}\left(M + \sin\theta\right)$$

$$\theta = \cos^{-1}\frac{\eta - z}{x-\xi}\beta$$

The downwash velocity is given by

$$v(x,z) = U\frac{\partial y_1}{\partial x} - i\omega y_1 \qquad \text{(A-18)}$$

Putting in equation A-14 and letting $L_1 = \pi$ as before, one obtains

$$v_{mn}(x,z) = A_{mn}\sin\frac{n\pi z}{L_2}\,\frac{U}{\pi}\sqrt{m^2\pi^2 - k^2}\left\{\cos(mx + \psi)\right\} \qquad \text{(A-19)}$$

Substituting $v(x,z)$, τ_1, and τ_2 into equation A-17 results in

$$\varphi(x,+0,z,t) = -A_{mn}\frac{U}{\beta\pi^2}\sqrt{m^2\pi^2 - k^2}\,e^{-i\omega t}\left\{\int_0^x \cos(m\xi + \psi)\,e^{i\omega\frac{\eta_0}{a\beta}M}\right.$$

$$\left.\int_0^{\pi}\sin\frac{n\pi}{L_2}\left(\eta_0\cos\theta + z\right)\cos\left(\frac{\omega\eta_0}{a\beta}\sin\theta\right)d\theta\,d\xi\right. \qquad \text{(A-20)}$$

To simplify the integrals in the above equation, let I_0 be defined by the following:

$$I_0 = \int_0^{\pi} \sin \frac{m\pi}{L_2}\left(\eta_0 \cos\theta + z\right) \cos\left(\frac{\omega \eta_0}{a\beta} \sin\theta\right) d\theta$$

$$= \cos \frac{m\pi z}{L_2} I_1 + \sin \frac{m\pi z}{L_2} I_2$$

where (A-21)

$$I_1 = \int_0^{\pi} \sin\left(\lambda \varkappa \cos\theta\right) \cos\left(\sigma \varkappa \sin\theta\right) d\theta$$

$$I_2 = \int_0^{\pi} \cos\left(\lambda \varkappa \cos\theta\right) \cos\left(\sigma \varkappa \sin\theta\right) d\theta$$

and

$$\varkappa = x - \xi$$

$$\lambda = \frac{m\pi}{L_2 \beta}$$

$$\sigma = \Omega / M$$

First consider I_1. Let $\theta = \Delta + \frac{\pi}{2}$. It is seen that

$$I_1 = -\int_{-\frac{\pi}{2}}^{\frac{\pi}{2}} \sin\left(\lambda \varkappa \sin\Delta\right) \cos\left(\sigma \varkappa \cos\Delta\right) d\Delta \qquad \text{(A-22)}$$

$$= 0$$

since the integrand is odd. Now consider I_2. Using the identities

$$\cos\left(\lambda \varkappa \cos\theta\right) = J_0(\lambda\varkappa) - 2J_2(\lambda\varkappa)\cos 2\theta + 2J_4(\lambda\varkappa)\cos 4\theta - \cdots \qquad \text{(A-23)}$$

$$\cos\left(\sigma \varkappa \sin\theta\right) = J_0(\sigma\varkappa) - 2J_2(\sigma\varkappa)\cos 2\theta + 2J_4(\sigma\varkappa)\cos 4\theta - \cdots$$

and the orthogonality relation,

$$\int_0^{\pi} \cos m\theta \cos m\theta \, d\theta = 0 \qquad m \neq m$$
$$= \frac{\pi}{2} \qquad m = m \qquad \text{(A-24)}$$

one obtains

$$I_2 = \pi J_0(\lambda\mathcal{H}) J_0(\sigma\mathcal{H}) - 2\pi J_2(\lambda\mathcal{H}) J_2(\sigma\mathcal{H}) + 2\pi J_4(\lambda\mathcal{H}) J_4(\sigma\mathcal{H}) - \cdots$$
$$= \pi N(\mathcal{H})$$

where

$$N(\mathcal{H}) = J_0(\lambda\mathcal{H}) J_0(\sigma\mathcal{H}) - 2J_2(\lambda\mathcal{H}) J_2(\sigma\mathcal{H}) + 2J_4(\lambda\mathcal{H}) J_4(\sigma\mathcal{H}) - \cdots$$

The resulting potential equation is

$$\varphi(x,+0,z,t) = -A_{mn} \frac{U}{2\pi\beta} \sqrt{m^2\pi^2 - k^2}\; e^{-i\omega t} e^{i\Omega x} \sin \frac{m\pi z}{L_2} \left\{ e^{i\psi} \varphi_M + e^{-i\psi} \varphi_N \right\} \qquad \text{(A-25)}$$

where

$$\varphi_M = \int_0^x e^{-i(\Omega - m)\xi} N(\mathcal{H}) \, d\xi$$

$$\varphi_N = \int_0^x e^{-i(\Omega + m)\xi} N(\mathcal{H}) \, d\xi$$

It can be shown that

$$\frac{\partial Q_M}{\partial x} = N(x) - i(\Omega - m) Q_M$$

$$\frac{\partial Q_N}{\partial x} = N(x) - i(\Omega + m) Q_N \qquad \text{(A-26)}$$

The pressure is

$$p_{mn} = A_{mn} \frac{U^2}{2\beta\pi^2} \sqrt{m^2\pi^2 - k^2}\; e^{-i\omega t}\, e^{i\Omega x}$$

$$\sin \frac{m\pi z}{L_z} \left\{ (m\pi - k)\, i e^{i\psi} Q_M - (m\pi + k)\, i e^{i\psi} Q_N \right. \qquad \text{(A-27)}$$

$$\left. + 2\pi (\cos\psi) N(x) \right\}$$

It is interesting to compare this result with the result of strip theory. If $J_0(\lambda R)$ is expanded in a series

$$J_0(\lambda R) = 1 - \left(\frac{\lambda R}{2}\right)^2 + \frac{\left(\frac{\lambda R}{2}\right)^4}{1^2 \cdot 2^2} \qquad \text{(A-28)}$$

and all powers of λ greater than the first are neglected (higher order Bessel functions are then completely neglected), then equation A-27 reduces to the strip theory solution, equation A-11. This is as would be expected since as $L_z \to \infty$, $\lambda \to 0$

c. Quasi-steady Theory

Another obvious simplification is to consider motion of small reduced frequency and assume that all terms of the equation involving the order k^2 or higher may be neglected. This has been worked out and is included in Appendix A.

B. Equations of Motion

The equations of motion for a rectangular plate such as that shown in Fig. 1 can be found using Lagrange's equations. Linear plate theory is used.

The normal modes in a vacuum for a simply supported plate are

$$q_{pls} \sin \frac{l\pi x}{L_1} \sin \frac{s\pi z}{L_2}$$

Taking q_{pls} as the generalized coordinates, so that

$$y(x,z,t) = \sum_{l} \sum_{s} q_{pls} \sin \frac{l\pi x}{L_1} \sin \frac{s\pi z}{L_2} \tag{B-1}$$

Lagrange's equations are

$$\frac{d}{dt}\left(\frac{\partial T}{\partial \dot{q}_{pls}}\right) + \frac{\partial V}{\partial q_{pls}} = Q_{ls} \tag{B-2}$$

Q_{ls} is the generalized aerodynamic force. The effect of edge loads in the plane of the plate may be included.

The kinetic energy is (Ref. 18)

$$T = \frac{\rho_s h}{2} \int_0^{L_1} \int_0^{L_2} \dot{y}^2 \, dx \, dz \tag{B-3}$$

$$= \frac{\rho_s h}{2} \frac{L_1 L_2}{4} \sum_{1}^{\infty} \sum_{1}^{\infty} (\dot{q}_{pmm})^2$$

The potential or strain energy consists of two parts--one due to bending and one due to tension or compression from the

edge loads. Consider the compressive loads S_1 and S_2 as shown in Fig. 5. Their contribution to internal strain energy is

$$V_T = -\frac{S_1}{2}\int_0^{L_1}\int_0^{L_2}\left(\frac{\partial y}{\partial x}\right)^2 dx\,dz - \frac{S_2}{2}\int_0^{L_1}\int_0^{L_2}\left(\frac{\partial y}{\partial z}\right)^2 dx\,dz$$

$$= -\frac{L_1 L_2 \pi^2}{8}\sum\sum q_{pqs}^2\left\{S_1\frac{q^2}{L_1^2} + S_2\frac{s^2}{L_2^2}\right\} \qquad \text{(B-4)}$$

The contribution from bending is

$$V_B = \frac{D}{2}\int_0^{L_1}\int_0^{L_2}\left\{\left(\frac{\partial^2 y}{\partial x^2}\right)^2 + \left(\frac{\partial^2 y}{\partial x^2}\right)^2 + 2\nu\,\frac{\partial^2 y}{\partial x^2}\frac{\partial^2 y}{\partial z^2} + 2(1-\nu)\left(\frac{\partial^2 y}{\partial x\,\partial z}\right)^2\right\} dx\,dz \qquad \text{(B-5)}$$

$$= \pi^4\frac{L_1 L_2}{8} D \sum_1^{\infty}\sum_1^{\infty}(q_{pqs})^2\left(\frac{q^2}{L_1^2} + \frac{s^2}{L_1^2}\right)^2$$

The total internal strain energy is

$$V = V_B + V_T$$

$$= \frac{\pi^2 L_1 L_2}{8}\left\{D\pi^2\sum_1^{\infty}\sum_1^{\infty} q_{pqs}^2\left(\frac{q^2}{L_1^2} + \frac{s^2}{L_2^2}\right)^2 - \sum_1^{\infty}\sum_1^{\infty} q_{pqs}^2\left(S_1\frac{q^2}{L_1^2} + S_2\frac{s^2}{L_2^2}\right)\right\} \qquad \text{(B-6)}$$

Inserting equation B-3 and B-6 into equation B-2 results in

$$\left[\ddot{q}_{pqs} + \omega_{qs}^2 q_{pqs}\right]\frac{\rho_s h L_1 L_2}{4} = Q_{qs} \qquad \text{(B-7)}$$

where

$$(\omega_{ls})^2 = \frac{\pi^2}{\rho_s h}\left\{ D\pi^2\left(\frac{l^2}{L_1^2} + \frac{s^2}{L_2^2}\right)^2 - \frac{S_1 l^2}{L_1^2} - \frac{S_2 s^2}{L_2^2} \right\}$$

ω_{ls} are the natural frequencies of the plate in a vacuum

ρ_s is the mass density of the plate

h is the plate thickness

$D = Eh^3/12(1-\nu^2)$, the plate flexural rigidity

Certain restrictions are placed upon S_1 and S_2. On the one hand, the yield stress of the material must not be exceeded if S_1 and S_2 impose tensile stresses. On the other hand, S_1 and S_2 must not exceed the critical buckling load for the plate. Since thin plates are under consideration this load may be quite small and as will be seen can be of great importance.

The equations of motion for a rectangular membrane are also of interest. The normal modes in a vacuum are the same as for the plate.

The kinetic energy is (Ref. 18)

$$T = \frac{\rho_s h}{2}\int_0^{L_1}\int_0^{L_2} (\dot{y})^2 \, dx\,dz$$

$$= \frac{\rho_s h}{2}\,\frac{L_1 L_2}{4}\sum_1^{\infty}\sum_1^{\infty} (\dot{q}_{pls})^2 \qquad \text{(B-8)}$$

Let S be the tension per unit length in the membrane, then the potential energy is

$$V = \frac{S}{2}\int_0^{L_1}\int_0^{L_2}\left\{\left(\frac{\partial y}{\partial x}\right)^2 + \left(\frac{\partial y}{\partial z}\right)^2\right\} dx\,dz$$

$$= \frac{S}{2}\pi^2\frac{L_1L_2}{4}\sum_1^\infty\sum_1^\infty\left(\frac{\ell^2}{L_1^2} + \frac{s^2}{L_2^2}\right) q_{\ell s}^2 \qquad \text{(B-9)}$$

Lagrange's equations become

$$\left[\ddot{q}_{\ell s} + \omega_{\ell s}^2 q_{\ell s}\right]\frac{\rho_s h L_1 L_2}{4} = Q_{\ell s} \qquad \text{(B-10)}$$

where

$$\omega_{\ell s}^2 = \frac{S\pi^2}{\rho_s h}\left(\frac{\ell^2}{L_1^2} + \frac{s^2}{L_2^2}\right)$$

The membrane equation of motion is the same as the plate equation except for the definition of $\omega_{\ell s}$. The generalized forces are the same for both. They will now be evaluated.

For simple harmonic motion

$$q_{\ell s} = A_{\ell s}\, e^{-i\omega t} \qquad \text{(B-11)}$$

The generalized forces, $Q_{\ell s}$, are by definition

$$Q_{\ell s}\delta A_{\ell s} = \sum_1^\infty\sum_1^\infty\int_0^{L_1}\int_0^{L_2} p_{mm}\,\delta A_{\ell s}\sin\frac{\ell\pi x}{L_1}\sin\frac{s\pi z}{L_2}\,dx\,dz \qquad \text{(B-12)}$$

It is convenient to define the following

$$\frac{Q_{ls}}{e^{-i\omega t}} = \frac{L_2}{2} \sum_{1}^{\infty} \sum_{1}^{\infty} A_{mn} Q_{mnls} \tag{B-13}$$

where

$$Q_{mnls} \quad \frac{2}{L_2} \int_0^{L_1} \int_0^{L_2} \frac{p_{mn}}{A_{mn} e^{-i\omega t}} \sin \frac{l\pi x}{L_1} \sin \frac{s\pi z}{L_2} \, dx \, dz$$

The equations of motion may now be written

$$\left[-\omega^2 + \omega_{ls}^2 \right] A_{ls} = \frac{2}{\rho_s h L_1} \sum_{1}^{\infty} \sum_{1}^{\infty} A_{mn} Q_{mnls} \tag{B-14}$$

a) Strip Theory

Q_{mnls} is defined by equation B-13. Substituting equation A-11 into equation B-13 and taking $L_1 = \pi$

$$Q_{mnls} = \frac{\rho a U^2}{\beta \pi^2 L_2} \sqrt{m^2\pi^2 - k^2} \int_0^{\pi} e^{i\Omega x} \left\{ 2\pi \cos \Psi \, J_0(\sigma x) \right.$$

$$- i(m\pi + k) e^{-i\Psi} Q_A \tag{B-15}$$

$$\left. + i(m\pi - k) e^{i\Psi} Q_B \right\} \sin lx \, dx \int_0^{L_2} \sin \frac{m\pi z}{L_2} \sin \frac{s\pi z}{L_2} \, dz$$

But

$$\int_0^{L_2} \sin \frac{m\pi z}{L_2} \sin \frac{s\pi z}{L_2} \, dz = 0 \qquad s \neq m$$

$$= \frac{L_2}{2} \qquad s = m \tag{B-16}$$

Thus Q_{mmls} has a value only when $s=m$. The subscripts m and s may be dropped since these integers no longer appear in the equation for Q_{mmls}. Thus

$$Q_{ml} = \frac{\rho_a U^2}{2\beta\pi}\sqrt{m^2\pi^2-k^2}\int_0^{\pi} e^{i\Omega x}\Big\{2\pi\cos\Psi\, J_0(\sigma x) - i(m\pi+k)e^{-i\Psi}\Phi_A + i(m\pi-k)e^{i\Psi}\Phi_B\Big\}\sin lx\, dx \tag{B-17}$$

The above integration can be performed with the result given in terms of the Schwarz function. After considerable manipulation the following is obtained.

For $m \neq l$

$$Q_{ml} = \frac{iml\rho_a U^2}{2\pi^2\beta(m^2-l^2)}\left\{\frac{(m\pi+k)^2}{m} I_{0\sigma}(m) - \frac{(m\pi-k)^2}{m} I_{0\sigma}(-m) + \frac{(l\pi+k)^2}{l} I_{0\sigma}(l) - \frac{(l\pi-k)^2}{l} I_{0\sigma}(-l)\right\} \tag{B-18}$$

for $m = l$

$$Q_{mm} = \frac{\rho_a U^2}{4\beta\pi^2}\left\{\frac{i}{m}(m^2\pi^2-k^2)\left[I_{0\sigma}(m) - I_{0\sigma}(-m)\right] + (m\pi+k)^2\pi\left[I_{0\sigma}(m) - I_{1\sigma}(m)\right] + (m\pi-k)^2\pi\left[I_{0\sigma}(-m) - I_{1\sigma}(-m)\right]\right.$$

where

$$I_{o\sigma}(b) = \int_0^{\pi} e^{i(\Omega+b)x} J_0(\sigma x)\, dx$$

$$= \pi \bar{f}_0\left(\frac{\Omega+b}{\sigma}, [\Omega+b]\pi\right)$$

$$I_{1\sigma}(b) = \frac{1}{\pi}\int_0^{\pi} e^{i(\Omega+b)x} \times J_0(\sigma x)\, dx \qquad \text{(B-19)}$$

$$= \pi \bar{f}_1\left(\frac{\Omega+b}{\sigma}, [\Omega+b]\pi\right)$$

The function f_1 is of the same family as f_0. It is defined as

$$f_1(a,b) = \frac{1}{b^2}\int_0^{b} e^{iu} J_0\left(\frac{u}{a}\right) u\, du \qquad \text{(B-20)}$$

In Ref. 16 a recurrence formula is given

$$\bar{f}_1(a,b) = \left(\frac{a^2}{a^2-1}\right)\frac{1}{b}\left\{\left[-i J_0\left(\frac{b}{a}\right) - \frac{1}{a} J_1\left(\frac{b}{a}\right)\right] e^{ib} + i \bar{f}_0(a,b)\right\} \qquad \text{(B-21)}$$

b) Exact Theory

By the same procedure used in the strip theory case Q_{mn} for the exact theory is found to be

$$Q_{m\ell} = \frac{\rho_a U^2}{2\beta\pi^2}\sqrt{m^2\pi^2 - k^2}\int_0^{\pi} e^{i\Omega x}\left\{2\pi\cos\Psi\, N(x) - i(m\pi + k)e^{-i\Psi} Q_N + i(m\pi - k)e^{i\Psi} Q_M\right\}\sin \ell x\, dx \tag{B-22}$$

With considerable work the above integration may be performed with results similar in form to equations B-18.

C. Flutter Determinant

Equations B-14 are the equations of motion for a simply supported rectangular plate with harmonic motion. It is assumed that the first few terms of the series expansion represent the flutter mode with sufficient accuracy. With this assumption the flutter condition becomes a finite determinant, since in order for equations B-14 to have a solution the determinant of the coefficients of A_{mn} must be zero. Thus

$$\Delta = \left| H_{mnls} \right| = 0 \qquad (C-1)$$

where

$$H_{mnls} = \left(-\omega^2 + \omega_{ls}^2\right) \delta_{mnls} - \frac{2}{\rho h L_1} Q_{mnls}$$

$$\delta_{mnls} = 1 \quad \text{if } m = l \text{ and } n = s$$

$$= 0 \quad \text{if } m \neq l \text{ or } n \neq s$$

Since in general the above determinant is complex valued it may be divided into real and imaginary parts both of which must vanish.

$$\Delta = \Delta_R + i\,\Delta_I = 0 \qquad (C-2)$$

Thus

$$\Delta_R = 0$$

$$\Delta_I = 0$$

Any two of the physical parameters may be solved by the above equations, given all the other parameters.

The problem can be simplified by writing equations B-14 in terms of the following non-dimensional parameters.

$$\frac{\omega L_1}{U} = k \qquad \frac{\omega_{ls} L_1}{U} = k_{ls}$$

$$\frac{Q_{mnls}}{\frac{1}{2}\rho_a U^2} = Q'_{mnls} \qquad \mu = \frac{\rho_a L_1}{\rho_s h} \tag{C-3}$$

Equations B-14 become

$$\left(-k^2 + k_{ls}^2\right) A_{ls} - \mu \sum_1^\infty \sum_1^\infty A_{mn} Q'_{mnls} = 0 \tag{C-4}$$

a) Strip Theory

For strip theory aerodynamics the equations of motion are

$$\left(-k^2 + k_{ls}^2\right) A_{ls} - \mu \sum_1^\infty A_{ms} Q'_{ml} = 0 \tag{C-5}$$

where Q'_{ml} is given by equation B-18.

The simplest approach is to consider only two terms of the series expansion as an approximation to the flutter mode. The choice of terms is important. For instance a plate deflection of the following form

$$\bar{y}(x,z) = A_{11} \sin \frac{\pi x}{L_1} \sin \frac{\pi z}{L_2} + A_{21} \sin \frac{2\pi x}{L_1} \sin \frac{\pi z}{L_2} \tag{C-6}$$

can be taken. The first term represents a half sine wave in both the X and Z directions. The second term represents a full

sine wave in the X direction, which is the direction of flow, and 1 half wave in the Z direction perpendicular to the flow. In the following numerical calculations only one half wave in the z direction is considered. It is felt that the shape in the direction parallel to the flow is far more important.

The determinant obtained from 2 modes as in equation C-6 is

$$\begin{vmatrix} \left(-k^2+k_{11}^2\right)-\mu Q_{11}' & -\mu Q_{21}' \\ -\mu Q_{12}' & \left(-k^2+k_{21}^2\right)-\mu Q_{22}' \end{vmatrix} = 0 \qquad \text{(C-7)}$$

By defining

$$x = \frac{k^2}{k_{11}^2} \qquad y = \frac{\mu}{k_{11}^2} = \frac{\mu x}{k^2} \qquad \text{(C-8)}$$

the determinant may be written

$$\begin{vmatrix} (1-x)-yQ_{11}' & -yQ_{21}' \\ -yQ_{12}' & \left(\frac{k_{21}}{k_{11}}\right)^2-x-yQ_{22}' \end{vmatrix} = 0 \qquad \text{(C-9)}$$

For 3 modes the term $A_{31} \sin \frac{3\pi x}{L_1} \sin \frac{\pi z}{L_2}$ is added to equation C-6. The determinant for 3 modes is

$$\begin{vmatrix} 1-x-yQ_{11}' & -yQ_{21}' & -yQ_{31}' \\ -yQ_{12}' & \left(\frac{k_{21}}{k_{11}}\right)^2-x-yQ_{22}' & -yQ_{32}' \\ -yQ_{13}' & -yQ_{23}' & \left(\frac{k_{31}}{k_{11}}\right)^2-x-yQ_{23}' \end{vmatrix} = 0 \qquad \text{(C-10)}$$

The reduced frequency ratios in the above can be determined from equation B-7. If aspect ratio is defined as

$$AR = \frac{L_2}{L_1} \tag{C-11}$$

then equation B-7 can be written

$$\omega_{ms}^2 = \frac{\pi^2}{L_1^2 \rho_s h}\left\{\frac{D\pi^2}{L_1^2}\left(m^2 + \frac{s^2}{AR^2}\right)^2 - \left(S_1 m^2 + S_2 \frac{s^2}{AR^2}\right)\right\} \tag{C-12}$$

The frequency ratios, $\left(\frac{k_{mi}}{k_{11}}\right)^2$, are

$$\left(\frac{k_{mi}}{k_{11}}\right)^2 = \frac{\frac{D\pi^2}{L_1^2}\left(m^2 + \frac{1}{AR^2}\right)^2 - \left(m^2 S_1 + \frac{S_2}{AR^2}\right)}{\frac{D\pi^2}{L_1^2}\left(1 + \frac{1}{AR^2}\right)^2 - \left(S_1 + \frac{S_2}{AR^2}\right)} \tag{C-13}$$

The unknown parameters in the above determinant are the Mach number, M ; density ratio, μ ; reduced frequency, k ; and reduced natural frequency, k_{mn} . For a plate of a given material, thickness, and chord length the k_{mn}'s are functions of aspect ratio, AR ; and edge compression, S_1 , and S_2 . With AR and S_1 and S_2 known all the higher k_{mn}'s can be expressed in terms of k_{11} by use of equation C-13. This leaves four unknown parameters in the above determinants. Due to the complexity of the calculations it is most convenient to assume values for M and k and to solve for μ and k_{11} .

The change in value of the frequency ratios resulting from a change in AR and edge compression has a very important effect on the flutter boundary. These ratios are given by equation C-13.

In order to illustrate the effect of AR on these ratios consider the case $S_1 = S_2 = 0$. The frequency ratios are

$$\left(\frac{K_{m1}}{K_{11}}\right)^2 = \left(\frac{AR^2 m^2 + 1}{AR^2 + 1}\right)^2 = \left(1 + \frac{m^2 - 1}{1 + \frac{1}{AR^2}}\right)^2 \qquad \text{(C-14)}$$

In Fig. 6 $\left(\frac{K_{m1}}{K_{11}}\right)$ vs. AR is plotted for the first four ratios. As $AR \to 0$, $K_{m1}/K_{11} \to 1$. It should be noted that for a given plate thickness and chord length, K_{11} gets large as AR gets small.

The effect of edge compression will now be discussed. It was previously mentioned that S_1 and S_2 must not exceed the critical buckling load. The relation for this buckling load is given in Ref. 19.

$$S_1 m^2 + S_2 \frac{m^2}{AR^2} = \frac{D\pi^2}{L_1^2}\left(m^2 + \frac{m^2}{AR^2}\right)^2 \qquad \text{(C-15)}$$

where m is the number of half waves in the x direction; n is the number in the z direction. The corresponding deflection of the buckled plate is given for any m and n by

$$y_{mn} = a_{mn} \sin \frac{m\pi x}{L_1} \sin \frac{n\pi z}{L_2} \qquad \text{(C-16)}$$

For $m = n = 1$

$$\left(S_1 + \frac{S_2}{AR^2}\right)_{CR} = \frac{D\pi^2}{L_1^2}\left(1 + \frac{1}{AR^2}\right)^2 \qquad \text{(C-17)}$$

Comparing equation C-17 with equation C-13 it is seen that as S_1 and S_2 approach the buckling load for $m = n = 1$

the denominator of equation C-13 approaches zero. If the mode for $m = n = 1$ is the lowest buckling mode then as the applied edge compression, $S_1 + S_2/AR^2$, approaches the buckling load $\left(S_1 + S_2/AR^2\right)_{CR}$ the frequency ratios get very large. To illustrate consider the specific case $AR = \infty$.

Define

$$R = \frac{S_1}{S_{CR}} \tag{C-18}$$

$S_{CR} = \frac{D\pi^2}{L_1^2}$ from equation C-17.

The frequency ratios are

$$\left(\frac{K_{m1}}{K_{11}}\right)^2 = \frac{m^2(m^2 - R)}{(1-R)} \tag{C-19}$$

The first four ratios are plotted in Fig. 7. Negative values of R refer to tensile loads.

However, if the first buckling mode does not give the lowest buckling load the results will be somewhat different. As an example consider a plate with $AR = 1$. The buckling mode $m = n = 1$ gives the critical load

$$\left(S_1 + S_2\right)_{CR} = \frac{4D\pi^2}{L_1^2} \tag{C-20}$$

This is the lowest load within the range

$$\frac{7D\pi^2}{L_1^2} \geq S_2 \geq -\frac{3D\pi^2}{L_1^2}$$

See Ref. 19, page 334.

For example with R defined as

$$R = \frac{S_1 + S_2}{(S_1 + S_2)_{CR}} \tag{C-21}$$

buckling occurs at $R = 1$. The frequency ratios for two possible cases say $S_2 = 0$ and $S_1 = 0$ are

$$\left(\frac{K_{m1}}{K_{11}}\right)^2 = \frac{\left(\frac{m^2+1}{2}\right)^2 - m^2 R}{1-R} \qquad S_2 = 0$$

$$\left(\frac{K_{m1}}{K_{11}}\right)^2 = \frac{\left(\frac{m^2+1}{2}\right)^2 - R}{1-R} \qquad S_1 = 0 \tag{C-22}$$

Equations C-22 are plotted in Fig. 8 for $m = 2, 3, 4$. If, however, the condition

$$S_2 < \frac{-3D\pi^2}{L_1^2} \tag{C-23}$$

is imposed, the lowest buckling load occurs for the mode $m = 2$ $m = 1$. Take for example

$$S_2 = -\frac{10D\pi^2}{L_1^2} \tag{C-24}$$

Then the buckling load is

$$(4S_1 + S_2)_{CR} = \frac{25D\pi^2}{L_1^2} \tag{C-25}$$

Define R so that $R=1$ corresponds to the critical buckling load above.

$$R = \frac{4S_1 + S_2}{\frac{25D\pi^2}{L_1^2}} \tag{C-26}$$

The frequency ratios are

$$\left(\frac{\lambda_{m1}}{\lambda_{11}}\right)^2 = \frac{(m^2+1)^2 + 7.5 - 6.25R}{11.5 - 6.25R} \qquad (C-27)$$

This is plotted in Fig. 9. The ratios do not change as much with R as in the preceding two examples.

The above cases were given to illustrate the change in frequency ratios with aspect ratio and edge compression. Each case must be investigated separately.

The frequency ratios of a membrane also are of interest. From equation B-10

$$\left(\frac{\lambda_{m1}}{\lambda_{11}}\right)^2 = 1 + \frac{m^2-1}{1+\frac{1}{AR^2}} \qquad (C-28)$$

The importance of these ratios is in their effect on the stability of the system. This is discussed in the next section.

D. Discussion of Results

Numerical calculations have been made for several cases. A two mode solution for $M=2$, $S_1 = S_2 = 0$, and for a range of AR's has been done with the results plotted in Fig. 10. The results of a 3 mode solution for the same range of parameters are plotted in Fig. 11. A comparison of the 2 and 3 mode solutions is presented in Fig. 12.

From intuitive argument the region below each curve is stable while above the curve it is unstable. This agrees with the energy criteria of Ref. 1.

These figures indicate a rather large change in the region of stability with change in AR, but it must be noted that for a plate of given material and thickness the value of K_{11} also changes as the aspect ratio is changed. An interesting way to plot the data is as follows:

$$K_{11}^2 = \frac{D\pi^4}{\rho_3 h L_1^2 U^2}\left(1 + \frac{1}{AR^2}\right)^2$$

Use (D-1)

$$K_{11}\Big/_{1+\frac{1}{AR^2}} = \frac{\pi^2}{L_1 U}\sqrt{\frac{D}{\rho_3 h}}$$

for the abscissa. For a plate of given material and chord length a plot of this sort will show the stability boundaries as a function of plate thickness. Fig. 13 is a replot of the $M=2$, 3 mode solution with $S_1 = S_2 = 0$ using the new abscissa. This figure shows the increasing stability for a given plate with decrease in aspect ratio.

The two mode solution for $M = \sqrt{2}$, $S_1 = S_2 = 0$, and for a range of AR's is presented in Figs. 14 and 15. For $M = \sqrt{2}$ two branches to the flutter boundaries appear for each aspect ratio. According to Ref. 1 the region between the two curves is stable while the region above the upper curve and below the lower curve is unstable. The lower branch disappears for sufficiently large values of K_{11}. See Ref. 4 for a further discussion of this.

For the membrane at $M = 2$, $AR = \infty$ no solution exists if 3 modes are considered. This agrees with the conclusions reached in Ref. 3.

It is also interesting to note that no solution exists for $M = 2, AR = \frac{1}{2}, S_1 \; S_2 \; O$ for 3 modes. The only differences in the flutter determinants for a change in AR are the changes in the frequency ratios. These changes are given in Fig. 6. For a given plate the greater instability with increasing AR shown in Fig. 13 can be associated with increasing differences in the frequency ratios. The fact that no solution exists for the membrane or $AR = \frac{1}{2}$ plate mentioned above indicates that for frequency ratios sufficiently close together the system is stable. This leads to interesting consequences when edge compression is considered since it also affects the frequency ratios. Nothing has been done to try to predict the stability directly from the frequency ratios however.

Another factor which has not been completely established is the number of modes required for convergence of the flutter boundary. The immense amount of work has limited the work to 3 modes at this time. Fig. 12 indicates less change in going from 2 to 3 modes at the higher AR's (higher difference in frequency ratios) than for the lower AR's . It would be desirable to compute higher modes to check convergence.

PART II. FLUTTER OF A TWO-DIMENSIONAL BUCKLED PLATE WITH CLAMPED EDGES IN A SUPERSONIC FLOW

A. Representation of the Flutter Mode

In Ref. 10 the flutter of a two-dimensional buckled plate with simply supported edges has been considered. The approach used there can be carried over directly for use in the clamped edge case. The boundary conditions for the clamped case are

$$y(0,t) = y(L,t) = 0$$
$$\frac{dy}{dx}(0,t) = \frac{dy}{dx}(L,t) = 0 \qquad \text{(A-1)}$$

It is desired to represent the flutter modes of such a plate by a series of functions which satisfy the above boundary conditions. The functions first used by Iguchi (Ref. 11) have been selected for use here. They are of the form

$$F_p(\xi) = \xi(\xi-1)^2 + (-1)^p \xi^2 (\xi - 1) - \frac{1}{p\pi} \sin p\pi\xi \qquad \text{(A-2)}$$

$$\xi = \frac{x}{L}$$

The flutter mode is represented by

$$y(\xi) = \sum_{p=1}^{N} b_p F_p(\xi) \qquad \text{(A-3)}$$

The initial buckling mode for the buckled plate is represented by

$$y_o(\xi) = \sum_{p=1}^{N} a_p F_p(\xi) \qquad \text{(A-4)}$$

B. Equations of Motion

The equations of motion may be derived by using Lagrange equations. The kinetic energy is

$$T = \frac{L^3}{2}\int_0^1 \rho_s h\left[\dot{y}(\xi)\right]^2 d\xi$$

$$= \frac{L^3\rho_s h}{2}\sum_i\sum_j b_i b_j I_{ij}^{(0)} \tag{B-1}$$

where $I_{ij}^{(0)}$ is an integral of the following form

$$I_{mp}^{(r)} = \int_0^1 F_m(\xi)\frac{d^r}{d\xi^r}F_p(\xi)d\xi = (-1)^r I_{pm}^{(r)} \tag{B-2}$$

Integration of $I_{mp}^{(r)}$ has been carried out in Ref. 12 for several values of r.

The strain energy term is made up of two parts. One part is due to the compression loading in the plane of the plate and the other is due to the bending of the plate. The membrane forces play an important part and therefore cannot be neglected. Their contribution to strain energy is

$$U_a = \frac{(1-\nu^2)LH^2}{2Eh} \tag{B-3}$$

where H is the membrane force per unit width

$$H = H_0 + \frac{Eh}{2(1-\nu^2)}\int_0^1\left[\left(\frac{dy_0}{d\xi}\right)^2 - \left(\frac{dy}{d\xi}\right)^2\right]d\xi$$

$$= H_0 + \frac{Eh}{2(1-\nu^2)}\left[\sum_i\sum_j\left(b_i b_j - a_i a_j\right)I_{ij}^{(2)}\right]d\xi \tag{B-4}$$

H_o is the initial value of the membrane force. Remember that this initial condition is not an unstressed state.

The contribution of bending to the strain energy is

$$U_b = \frac{D}{2L}\int_0^1 (y'' - y_o'' - \frac{H_o}{D} y_o)^2 \, d\xi \qquad \text{(B-5)}$$

$$= \frac{D}{2L}\Big\{ \sum_i \sum_j (b_i - a_i)(b_j - a_j) I_{ij}^{(4)}$$

$$- \frac{2H_o L^2}{D} \sum_i \sum_j (b_i - a_i) a_j I_{ij}^{(2)}$$

$$+ \left(\frac{H_o L^2}{D}\right)^2 \sum_i \sum_j a_i a_j I_{ij}^{(0)}$$

Putting the above into Lagrange's equations

$$\frac{d}{dt}\left(\frac{\partial T}{\partial \dot{b}_i}\right) + \frac{\partial (U_a + U_b}{\partial b_i} = Q_i \qquad \text{(B-6)}$$

results in

$$L^3 \rho_s h \sum_j \ddot{b}_j I_{ij}^{(0)} + L\Big\{ H_o + \frac{Eh}{2(1-\nu^2)} \Big[\sum_i \sum_j (b_i b_j$$

$$- a_i a_j) I_{ij}^{(2)} \Big] \Big\} \Big\{ \sum_j b_j I_{ij}^{(2)} \Big\} + \frac{D}{L} \Big\{ \sum_j (b_j - a_j) I_{ij}^{(4)}$$

$$- \frac{H_o L^2}{D} \sum_j a_j I_{ij}^{(2)} \Big\} = Q_i \qquad \text{(B-7)}$$

Q_i is the generalized force.

C. Aerodynamic Forces

If the quasi-steady simplifying assumption is used the aerodynamic pressure is (Ref. 10)

$$p(\xi,t) = \frac{\rho_a U^2}{\sqrt{M^2-1}} e^{i\omega t} \left\{ \frac{\partial y(\xi)}{\partial \xi} + ik\left(\frac{M^2-2}{M^2-1}\right) y(\xi) + \frac{ik}{M^2-1} y(0) \right\} \qquad (C-1)$$

The generalized force is given by

$$Q_i = -L^2 \int_0^1 p(\xi) F_i(\xi) d\xi \qquad (C-2)$$

Substituting for the deflection and then inserting the resulting expression for the pressure into the equation above results in

$$Q_i = -\frac{\rho_a U^2 L^2}{\sqrt{M^2-1}} \left\{ \sum_j b_j I_{ij}^{(1)} + \frac{\alpha L}{U} \sum_j \dot{b}_j I_{ij}^{(0)} \right\} \qquad (C-3)$$

$$\alpha = \frac{M^2-2}{M^2-1}$$

The above expression refers to flow over one surface of the plate. The other side is assumed to be vented to the free stream static pressure.

D. Reduction to Dimensionless Equations

Let

$$\lambda_i = \frac{a_i \sqrt{3(1-\nu^2)}\, L}{c_i h} = i^{th} \text{ component of initial arch}$$

$$B_i = \frac{b_i \sqrt{3(1-\nu^2)}\, L}{c_i h} = i^{th} \text{ component of deflection curve}$$

$$S_c = \frac{H_0 L^2}{41.18\, D} = \text{membrane compression stress ratio} \qquad (D-1)$$

$$Q = \frac{\rho_a U^2 L^3}{D\pi^4\sqrt{M^2-1}} = \text{dynamic pressure ratio}$$

$$\gamma = \sqrt{M^2-1}\,\frac{\rho_s h}{\rho_a L} = \text{mass ratio} \qquad \text{(D-1 cont'd)}$$

$$\tau = \frac{Ut}{L} = \text{dimensionless time}$$

The constant c_i has been introduced in λ_i and B_i. It is chosen so that

$$\left[c_i F_i(\xi)\right]_{MAX} = 1 \qquad \text{(D-2)}$$

This has been done so that λ_i and B_i will refer directly to the amplitude of the mode. In the simply supported case $c_\tau = 1$ since

$$\left[\sin m\pi\xi\right]_{MAX} = 1$$

Upon substituting the above into the equations of motion there results

$$Q\pi^4\gamma \sum_j \frac{\partial^2 B_j}{\partial\tau^2} c_j I_{ij}^{(0)} + Q\pi^4\alpha \sum_j \frac{\partial B_j}{\partial\tau} c_j I_{ij}^{(0)}$$

$$+ Q\pi^4 \sum_j B_j c_j I_{ij}^{(1)} + 41.18\, S_c \sum_j (B_j - \lambda_j) c_j I_{ij}^{(2)}$$

$$+ \frac{2}{(1-\nu^2)}\left[\sum_j \sum_i (B_i B_j - \lambda_i \lambda_j) c_i c_j I_{ij}^{(2)}\right]\left[\sum_j B_j c_j I_{ij}^{(2)}\right]$$

$$+ \sum_j (B_j - \lambda_j) c_j I_{ij}^{(4)} = 0 \qquad \text{(D-3)}$$

Since uniform plates which are flat in the unstressed state are considered, the initial condition is the first mode of buckling. H_o is the buckling load for the first mode. If the first term of the series for $y_o(\xi)$ is assumed to be the first buckling mode, then

$$H_o = \frac{41.18\,D}{L^2} \qquad \text{and} \qquad S_c = 1 \tag{D-4}$$

For convenience introduce the notation

$$\chi = \frac{2}{41.18\,(1-\nu^2)}\left[\sum_j \sum_i \left(B_i B_j - \lambda_i \lambda_j\right) c_i c_j\, I_{ij}^{(2)}\right] \tag{D-5}$$

From equation B-4

$$H = H_o + \frac{2\,D}{(1-\nu^2)\,L^2}\left[\sum_j \sum_i \left(B_i B_j - \lambda_i \lambda_j\right) c_i c_j\, I_{ij}^{(2)}\right] \tag{D-6}$$

$$= H_o\,(1+\chi)$$

Thus χ can be interpreted as

$$\chi = \frac{H}{H_o} - 1 = \frac{\text{Compressive Load}}{\text{First Buckling Load}} - 1 \tag{D-7}$$

E. Approximation in Two Degrees of Freedom

In the initial condition all λ_i's for $i \geq 2$ are zero. If all B_i's for $i \geq 3$ are neglected then

$$\chi = \frac{2}{41.18\,(1-\nu^2)}\left[\left(B_1^2 - \lambda_1^2\right) c_1^2\, I_{11}^{(2)} + B_2^2\, c_2^2\, I_{22}^{(2)}\right] \tag{E-1}$$

The values for $I_{ij}^{(r)}$ obtained from Ref. 12 may be substituted into the various terms and two equations of motion follow

$$\gamma \frac{\partial^2 B_1}{\partial \tau^2} + \alpha \frac{\partial B_1}{\partial \tau} - 3.5038\, B_2 - 5.1554 \frac{\chi}{Q} B_1 = 0$$

$$\gamma \frac{\partial^2 B_2}{\partial \tau^2} + \alpha \frac{\partial B_2}{\partial \tau} + (19.964 - 19.174\chi) \frac{B_2}{Q} + 3.1635\, B_1 = 0 \qquad \text{(E-2)}$$

In all calculations the value $\nu^2 = 0.1$ is used.

F. Static Equilibrium

If the derivatives with respect to τ all vanish, equations E-2 have a solution for B_1 and B_2 only if the determinant of their coefficients is equal to zero. The solution of the determinant is

$$\chi = 0.5206\left(1 \pm \sqrt{1 - 0.41366\, Q^2}\right) \qquad \text{(F-1)}$$

χ becomes imaginary when

$$Q = 1.5548$$

so no static equilibrium other than $y(\xi) = 0$ exists when $Q > 1.5548$.

The condition for the plate to become flat when $Q < 1.5548$ is

$$Q = 0.10679\, c_1 \lambda_1 \left\{1.0 - 0.0011796\, c_1^2 \lambda_1^2\right\}^{\frac{1}{2}} \qquad \text{(F-2)}$$

The value of c_1 is

$$c_1 = -14.639$$

so that $\lambda_1 = 1.41$ when $Q = 1.5548$

Hence for

$$\lambda_1 < 1.41 \qquad Q_{CR} = 0.10679\, c_1 \lambda_1 \left\{ 1 - 0.0011796\, c_1^2 \lambda_1^2 \right\}^{1/2}$$

$$\lambda_1 > 1.41 \qquad Q_{CR} = 1.5548 \tag{F-3}$$

See Fig. 16 for a plot of Q_{CR} vs. λ_1.

G. Small Perturbations About Static Equilibrium

The first order perturbation equations which result from imposing small perturbations $\delta B_1, \delta B_2$ onto B_1 and B_2 in equation E-2 are,

$$\gamma \delta \ddot{B}_1 + \alpha \delta \dot{B}_1 + \left\{ -3.5038 + 11.175 \frac{B_1 B_2}{Q} \right\} \delta B_2$$

$$+ 5.1554 \left\{ 2B_1^2 - \chi \right\} \frac{\delta B_1}{Q} = 0$$

$$\gamma \delta \ddot{B}_2 + \alpha \delta \dot{B}_2 + \left\{ 19.964 + 41.561\, B_2^2 - 19.174\, \chi \right\} \frac{\delta B_2}{Q} \tag{G-1}$$

$$+ \left\{ \frac{10.092}{Q} B_1 B_2 + 3.1635 \right\} \delta B_1 = 0$$

where

$$\chi = 0.26316 \left\{ \lambda_1^2 - B_1^2 - 4.1183\, B_2^2 \right\} \tag{G-2}$$

If solutions of the form

$$\delta B_1 = A e^{\mu \tau} \qquad \delta B_2 = B e^{\mu \tau}$$

are assumed, two homogeneous equations are obtained. For a solution other than $\delta B_1 = \delta B_2 = 0$ to exist the determinant of

these must vanish. The determinant

$$\begin{vmatrix} \left(\gamma\mu^2 + \alpha\mu + \frac{5.1554}{Q}\left\{2B_1^2 - \chi\right\}\right) & \left(-3.5038 + 11.175\,\frac{B_1 B_2}{Q}\right) \\ \left(3.1635 + 10.092\,\frac{B_1 B_2}{Q}\right) & \left(\gamma\mu^2 + \alpha\mu + \left\{19.964 + 41.561\,B_2^2 - 19.174\chi\right\}\frac{1}{Q}\right) \end{vmatrix} = 0 \qquad \text{(G-3)}$$

Expanded this may be written

$$a_4\mu^4 + a_3\mu^3 + a_2\mu^2 + a_1\mu + a_0 = 0 \qquad \text{(G-4)}$$

where

$$a_4 = \gamma^2$$

$$a_3 = 2\alpha\gamma$$

$$a_2 = \left\{\frac{\alpha^2 Q}{\gamma} + 19.964 + 10.311\,B_1^2 + 41.561\,B_2^2 - 24.329\chi\right\}\frac{\gamma}{Q}$$

$$a_1 = \left\{19.964 + 10.311\,B_1^2 + 41.561\,B_2^2 - 24.329\chi\right\}\frac{\alpha}{Q}$$

$$a_0 = \frac{1}{Q^2}\left\{98.850\chi^2 - \left[214.26\,B_2^2 + 197.70\,B_1^2 + 102.92\right]\chi + 205.84\,B_1^2 + 315.75\,B_1^2 B_2^2 + 11.084\,Q^2\right\}$$

Routh's discriminant is defined as

$$R = a_1 a_2 a_3 - a_0 a_3^2 - a_4 a_1^2 \qquad \text{(G-5)}$$

The conditions for stability of the disturbed motion are that a_4, a_3, a_2, a_1, a_0 and R all have the same sign. The requirements for this reduce to (Ref. 10)

$$\alpha > 0 \qquad a_0 > 0 \qquad R > 0 \qquad \text{(G-6)}$$

Of special interest is the stability about the flat configuration

Let $B_1 = B_2 = 0$ and $\chi = 0.26316\,\lambda_1^2$

Then

$$a_0 = 98.850\frac{\chi^2}{Q^2} - 102.92\frac{\chi}{Q^2} + 11.084 \qquad \text{(G-7)}$$

The critical condition $a_0 = 0$ is identical to equation F-2.

R becomes

$$R = \frac{2\alpha^2\gamma^2}{Q^2}\left\{98.250\chi^2 + 279.86\chi + 177.31\,Q^2 + \frac{\alpha^2 Q}{\gamma}\left[19.964 - 24.329\chi\right]\right\}$$

The critical condition is $R = 0$. In Fig. 16 Q_{CR} vs. λ_1 is plotted for $R = 0$.

For this plot the values $\gamma = 60$, $\alpha = 0.7335$ ($M = 2.18$) were chosen. These values compare with values obtained in experimental tests which are discussed in Part III. In actuality the curve $R=0$ is very insensitive to changes in α and γ. The unstable areas lie on the shaded side of the curves $Q=0$ and $R=0$.

H. Flutter with Finite Amplitude

Assume that an essentially sinusoidal motion exists.

Let

$$B_1 = A_1 \sin(k\tau + \varphi_1) = A_1 \sin\theta_1$$

$$B_2 = A_2 \sin(k\tau + \varphi_2) = A_2 \sin\theta_2 \qquad \text{(H-1)}$$

where $A_1(\tau)$, $A_2(\tau)$, $\varphi_1(\tau)$, $\varphi_2(\tau)$ are showly varying functions of time. Substituting equations H-1 into the equations of motion, E-2, results in a set of first order differential equations for $A_1, A_2, \varphi_1, \varphi_2$ if the conditions

$$\frac{dA_1}{d\tau}\sin\theta_1 + \frac{d\varphi_1}{d\tau}A_1\cos\theta_1 = 0$$

$$\frac{dA_2}{d\tau}\sin\theta_2 + \frac{d\varphi_2}{d\tau}A_2\cos\theta_2 = 0 \qquad \text{(H-2)}$$

are imposed. The first of equations E-2 becomes

$$\gamma k\frac{dA_1}{d\tau} = f_1(A_1, A_2, \varphi_1, \varphi_2, k\tau)\cos\theta_1$$

$$\gamma k A_1\frac{d\varphi_1}{d\tau} = -f_1(\cdots)\sin\theta_1 \qquad \text{(H-3)}$$

where

$$f_1(\cdots) = A_1 \gamma k^2 \sin\theta_1 - A_1 \alpha k \cos\theta_1 + 5.1554 \frac{\chi}{Q} A_1 \sin\theta_1 + 3.5038 A_2 \sin\theta_2$$

The second of equations E-2 becomes

$$\gamma k \frac{dA_2}{d\tau} = f_2(\cdots)\cos\theta_2$$

$$\gamma k A_2 \frac{d\varphi_2}{d\tau} = -f_2(\cdots)\sin\theta_2 \qquad \text{(H-9)}$$

where

$$f_2(\cdots) = \gamma k^2 A_2 \sin\theta_2 - \alpha k A_2 \cos\theta_2 + \frac{(19.174\chi - 19.964}{Q} A_2 \sin\theta_2 - 3.1635 A_1 \sin\theta_1$$

For steady oscillations to exist the average values of $\frac{dA_1}{d\tau}$, $\frac{dA_2}{d\tau}$, $\frac{d\varphi_1}{d\tau}$, $\frac{d\varphi_2}{d\tau}$ over a period of motion must vanish, i. e.

$$\gamma k \overline{\frac{dA_1}{d\tau}} = \frac{1}{2\pi}\int_0^{2\pi} f_1(\cdots)\cos\theta_1 \, d(k\tau) = 0$$

$$\gamma k \overline{A_1 \frac{d\varphi_1}{d\tau}} = \frac{1}{2\pi}\int_0^{2\pi} f_1(\cdots)\sin\theta_1 \, d(k\tau) = 0 \qquad \text{(H-5)}$$

$$\gamma k \overline{\frac{dA_2}{d\tau}} = \frac{1}{2\pi}\int_0^{2\pi} f_2(\cdots)\cos\theta_2\, d(k\tau) = 0$$

$$\gamma k \overline{A_2 \frac{d\varphi_2}{d\tau}} = \frac{1}{2\pi}\int_0^{2\pi} f_2(\cdots)\sin\theta_2\, d(k\tau) = 0$$

The four resulting equations are

$$-\alpha k A_1 + 1.3968\frac{A_1 A_2^2}{Q}\sin 2\varphi - 3.5038\, A_2 \sin\varphi = 0$$

$$-\alpha k A_2 - 1.2615\frac{A_2 A_1^2}{Q}\sin 2\varphi - 3.1635\, A_1 \sin\varphi = 0$$

$$\gamma k^2 A_1 + 1.3567\frac{A_1}{Q}\left\{\lambda_1^2 - \frac{3}{4}A_1^2 - 1.0296\left(2A_2^2 + A_2^2\cos 2\varphi\right)\right\} + 3.5038\, A_2\cos\varphi = 0$$

$$\gamma k^2 A_2 + 1.2615\frac{A_2}{Q}\left\{4\lambda_1^2 - 2A_1^2 - A_1^2\cos 2\varphi - 12.355\, A_2^2 - 19.964\frac{A_2}{Q}\right\} - 3.1635\, A_1\cos\varphi = 0 \qquad \text{(H-6)}$$

where $\varphi = \varphi_1 - \varphi_2 = \theta_1 - \theta_2$

Equations H-6 are to be solved for A_1, A_2, φ, and k for a given set of values for $\gamma, Q, \alpha, \lambda_1$. In practice this is very difficult but the problem of finding λ_1, k, Q, and α from a given set of γ, A_1, A_2, and φ is straightforward. Equations H-6 may be rearranged as follows

$$Q = -\frac{\left\{1.3968\,A_2^2 + 1.2615\,A_1^2\right\}}{\left\{3.1635\,A_1^2 - 3.5038\,A_2^2\right\}}\,2A_1A_2\cos\varphi$$

$$3.6893\,\lambda_1^2 = 1.5055\,A_1^2 + 19.964 + A_2^2\left\{18.299 + 1.3567\cos 2\varphi\right\} + Q\cos\varphi\left\{3.5038\,\frac{A_2}{A_1} + 3.1635\,\frac{A_1}{A_2}\right\} \qquad \text{(H-7)}$$

$$k^2 = -\frac{1.3567}{\gamma Q}\left\{\lambda_1^2 - \frac{3}{4}A_1^2 - 1.0296\left(2A_2^2 + A_2^2\cos 2\varphi\right)\right\} + \frac{3.5038}{\gamma}\,\frac{A_2}{A_1}\cos\varphi$$

$$\alpha = -\frac{8.8388\,A_1A_2\sin\varphi}{\left\{1.2615\,A_1^2 + 1.3968\,A_2^2\right\}k}$$

For selected values of A_1, A_2, φ, and γ it is possible to solve for Q, λ_1, k, and α in that order. Since Q, λ_1, and k must be real and positive to have physical meaning flutter boundaries may be obtained. Some numerical calculations have been made for $A_2 = 0.5$, 0.8, and 1.0; $\gamma = 60$; $0 < A_1 < 10$; $\pi/2 < |\varphi| < \pi$. For a given Mach number flutter is possible under certain combinations of A_2, A_1, φ, and γ. In Table I the results of some specific calculations are presented. The Mach number, $M = 2.18$,

and mass ratio, $\gamma = 60$, were selected to correspond to values used in some experimental tests discussed in Part III.

The results of Q vs λ_1 for $M = 2.18$, $\gamma = 60$, and $A_2 = 0.5$, 0.8, 1.0 are plotted in Fig. 16. For each A_2 a series of points have been found--each point corresponding to a given φ. These results show flutter can occur for values of φ up to the limiting case of $|\varphi| = \pi$. For values of $|\varphi| < \pi$ the curve for a given A_2 goes up and to the right and then down as illustrated in Fig. 16. Each value of A_2 has a loop of this type. Any point on this loop gives the possible flutter mode and frequency for the specific values of $\gamma, A_2, Q, \lambda_1$. By taking a large number of A_2's it is possible to establish the pattern for all pairs of parameters, Q and λ_1, where there exists a solution of the nature of a limiting cycle that is approximated by a two mode expansion. Such solutions exist to the right of the boundary as shown in Fig. 16 for $M = 2.18$, $\gamma = 60$. To the left of this boundary a solution of the assumed form does not exist. If flutter of finite amplitude exists at all for a Q and λ_1 to the left of the boundary either the flutter mode may not be expressed by the first two terms of the series expansion of Eq. A-3 or the limit cycle is not nearly harmonic as assumed in Eq. H-1.

PART III. EXPERIMENTAL STUDY OF THE FLUTTER OF A TWO-DIMENSIONAL BUCKLED PLATE WITH CLAMPED EDGES IN A SUPERSONIC FLOW

A. Purpose of Test

The primary purpose of the test was to study the nature of panel flutter. From this information present theoretical methods could be checked and perhaps new approaches could be suggested. With this purpose in mind an experiment was designed to provide information regarding the mode shape of the flutter; the accuracy with which the motion could be approximated by harmonic motion; the frequency of the flutter; and the combination of parameters which formed the boundary between a region of flutter and a region with no flutter. On the following pages the model, instrumentation, test procedure, and results are discussed.

B. Model and Instrumentation

In order to establish a range of parameters, if any, in which panel flutter existed preliminary tests were conducted in the Caltech $2\frac{1}{2}$ inch supersonic wind tunnel. These preliminary tests, while not productive of any good quantitative results, were invaluable in supplying information for the design and instrumentation of a larger model.

The main tests were conducted in the Caltech JPL 12 inch supersonic wind tunnel. A tunnel of this size made it possible to use standard structural sizes of aluminum for the panels. A flat plate model was designed to hold the panel. This model is illustrated in Fig. 17. The model was mounted on the centerline of the tunnel with the upper surface parallel to the airflow.

As illustrated in Fig. 17 the panel is fastened flush with the upper surface of the model. It is located near the leading edge to minimize the effects of boundary layer. The leading and trailing edges of the panel are fastened with screws as shown in Sections A-A and B-B of Fig. 17. This was to provide a close approximation to a clamped end condition consistent with easy removal of the panel. The side edges are free. The lower surface of the panel is vented to the free stream static pressure by the slits along the free edges.

A combination screw, wedge, and slide arrangement is used to buckle the panel by moving the trailing edge with respect to the leading edge. This is illustrated in Sections B-B and C-C of Fig. 17. The slide permits horizontal motion but restrains the trailing edge in rotation. With proper adjustment the resulting deflection is a pure buckling deflection. To buckle the panel the two wedges illustrated in Section C-C of Fig. 17 are moved together by turning the operating rod by the right hand screw convention. This forces the slide forward and buckles the panel. The operating rod passes through the sidewall of the tunnel so that the plate may be buckled from outside the tunnel while the tunnel is running. To decrease the amount of buckle the rod is turned to the left. Springs are provided to aid in the return of the slide.

The amount of buckle was measured by the position of the rod which moves the wedges. It was calibrated by placing a dial gage at the center of the plate and measuring the amount

of deflection from the flat configuration for various degrees of rotation of the rod.

Several SR-4 strain gages were fastened to the lower surface of the panels equally spaced along the centerline. The signal from the gages was fed into a Miller recording oscillograph for a permanent record. No attempt was made to calibrate the amplitude of the trace with the amount of strain. Instead each gage was set so that for a given strain each trace would record the same amplitude. In this way relative values of strain along the length of the panel could be determined but not absolute values.

All panels were approximately 11 inches long and 11 inches wide. Several thicknesses were tested from 0.025 inches to 0.051 inches. The free edges were $\frac{1}{2}$ inch from the tunnel sidewalls. The slits along the free edges were approximately 1/16 inch wide.

C. Test Procedure

The significant parameters which could be varied in the wind tunnel test are Mach number; plate material and thickness; tunnel static pressure; and the amplitude of buckle. Due to the short time available for the test the number of variations in the parameters had to be kept to a minimum. Only one Mach number, $M \approx 2.18$, was used. Several thicknesses of 24 ST aluminum panels were prepared. It was possible to vary the tunnel supply pressure from 1 atmosphere up to approximately 2 atmospheres. It was possible to vary the amplitude of buckle from zero up to about 12 panel thicknesses depending on the panel tested.

The standard procedure used for the tests was as follows:

1) A panel of given thickness was selected and installed. The gages were connected and the amplifiers and oscillograph were checked.

2) The tunnel was started and a short time was allowed for the flow to stabilize.

3) A supply pressure for the wind tunnel was selected. For the first run this was usually set at one atmosphere.

4) The panel was then buckled and the amplitude was gradually increased until flutter occurred or until it reached the maximum amplitude possible with this model.

5) When flutter occurred the oscillograph was started and a time history of the motion was recorded. The flutter was stopped by decreasing the amplitude.

6) The pressure was then changed and steps 4 and 5 were repeated.

7) When a full range of pressures and amplitudes had been checked, a new panel was selected and steps 1 through 6 were repeated.

One of the variations of the above was to start the oscillograph before the flutter started and to keep it on until the flutter was stopped.

D. Results of Test

Four thicknesses of panels were tested. The thickest, an 0.051 inch panel, would not flutter under any combination of pressure and buckling amplitude available. The 0.040 inch panels fluttered in certain cases at the higher pressures and amplitudes. The 0.031 inch panels fluttered over a wide range of pressures and amplitudes.

Two of these plates gave the most significant results. The 0.025 inch panels fluttered at the lowest pressures possible (1 atmosphere supply pressure) even with no buckling load.

Two distinct types of flutter were observed. One occurred at much lower amplitudes of the buckle, λ_1, than the other. Hereafter it will be referred to as low amplitude flutter. Its characteristics are definitely different from the other, large amplitude type.

The results of the tests are presented in Table II. The dimensionless parameters Q, λ_1, and γ as defined in equation D-1, Part II, have been calculated and are included in Table II. The type of flutter is of the large amplitude type unless marked otherwise.

The results of Q_{CR} vs. λ_1 are plotted in Fig. 18. The low amplitude flutter is marked by a dash through the line. The reason for using a line to indicate the amplitude, λ_1, at which flutter occurred is due to the uncertainty in the measurement of λ_1. The amplitude of buckle was calibrated before and after each run. Usually there was a zero shift which accounts for the length of the line.

Two sections of the oscillograph tape are shown in Fig. 19. The first, marked Trace 275, shows the large amplitude flutter. A short section of trace showing the panel at rest but with the tunnel running is also shown. Seven gages were fastened at equal intervals along the centerline of the plate. Gage number 1 was not working so no trace exists. The gages were numbered in sequence from front to rear. Gage 4 is at the middle of the plate. The dominant motion is quite evident. Superimposed

upon it is a higher frequency motion. This motion definitely existed and was not in the instrumentation. The timing marks are at each one-hundredth of a second.

The second, Trace 131, is of the low amplitude type. The motion here has a very different character which will be discussed later.

The oscillograph recordings such as the above mentioned traces are in effect measures of the plate curvature. By performing a double integration the deflection may be determined. The resulting deflection shapes are shown in Fig. 20 for Trace 275 and in Fig. 21 for Trace 131. Note the traveling wave nature of the motion in Trace 275. The ordinate has no value assigned since the gages are calibrated only to read relative amplitudes. The times listed for each successive drawing are measured from an arbitrary zero. Only the dominant motion is considered.

In Part II the deflection of the panel was represented by a series of Iguchi functions. If only the first two terms are considered, the deflection is of the following form

$$Y(\xi) = \Theta_1 C_1 F_1(\xi) + \Theta_2 C_2 F_2(\xi) \qquad \text{(D-1)}$$

Θ_1 and Θ_2 have been evaluated for Trace 275 and the results are plotted in Fig. 22. No values have been assigned to the ordinate since only the relative values of Θ_1 and Θ_2 have significance. From this plot the amplitude ratio, Θ_1/Θ_2 , and the phase shift, φ , may be determined. A sine curve has been superimposed on this plot for comparison.

In Fig. 23 the results of low amplitude motion, Trace 131, are presented. The results of another large amplitude motion, Trace 283, are shown in Fig. 24. In all three cases the time scales are measured in seconds from an arbitrary zero. In the case of Trace 283, however, the plate is buckled but at rest at $t = 0$ and is followed through the start of the motion and through one complete cycle.

E. Conclusions

The results plotted in Fig. 18 show only a slight variation in Q_{CR} with change in λ_1. This change is most pronounced in the large amplitude range. At amplitudes, λ_1, greater than approximately 6 there is a definite decrease in Q_{CR} with increase in λ_1. In the low amplitude range the change of Q_{CR} with amplitude is not so clear. It was in evidence, however, in the following manner:

In a typical test the tunnel was set at some pre-selected Q with the panel in the unbuckled condition. The panel was then buckled and the amplitude was slowly increased. At some point low amplitude flutter was observed. With further increase in amplitude, λ_1, the flutter stopped. With a still larger amplitude a point was reached at which large amplitude flutter occurred. At no time did flutter stop at larger amplitudes than those required for initiating large amplitude flutter. In most cases it was not possible to keep increasing the amplitude because of mechanical limitations. For examples of the test described above see Traces number 162 and 163; 180 and 181; and 285 and 288. In

other cases, particularly those which required very large amplitude to initiate flutter, no low amplitude flutter was observed.

The possibility exists of a combination of Q and λ_1 for which the flutter started as a low amplitude type and changed to large amplitude type as λ_1 was increased without a stable region in between. Additional tests would be required to investigate this.

The various stability boundaries presented in Fig. 16 and discussed in Part II are replotted in Fig. 18. It is difficult to draw conclusions concerning the validity of the theoretical curves in predicting the flutter boundaries. The large amplitude flutter occurred in a region permitted by the two mode solution of Part II. No large amplitude flutter occurred to the left of this curve in the region where the two mode solution indicates no solution exists. This curve does not seem to have significance with regard to the low amplitude flutter since this type of flutter was observed on both sides. If higher modes are considered, some correlation may be found.

No flutter was observed for values of Q below the curve for stable static buckling as presented in equation F-3, Part II. However there is a definite gap between the experimental points and the theoretical curve. Assuming that this curve is a valid boundary the discrepancy could result from a combination of the following factors.

1) The boundary conditions on the panel do not exactly represent the clamped end conditions.

2) The panels are theoretically under a pure buckling load. In the manufacture of the model the necessary tolerances permit a slight amount of initial curvature which induces additional stresses.

3) A panel of finite width was used. This may not adequately approximate the two-dimensional condition.

4) The free edges were extended slightly into the boundary layer on the sidewalls of the tunnel. This edge effect may be important.

5) The boundary layer on the panel was ignored in the theoretical study. For small oscillations it is possible for the flutter to take place entirely within the boundary layer. The panel was placed near the model leading edge to minimize this effect.

6) The dead air space below the panel was restricted by the maximum permissible thickness of the model.

It would be desirable to check all the above conditions and some others to determine their effect. The short time allotted for testing completely precluded the possibility of checking these factors. The tests of necessity had to be primarily concerned with two questions: Does flutter occur? If so, what does it look like? The information concerning flutter boundaries could at best be incomplete.

In regions of small initial amplitudes the position of the experimental points is uncertain. It was very difficult to measure λ_1 for small deflections due to the shift in the zero. In

all cases recorded in Table II the panel was definitely buckled although in several cases it was impossible to determine the size of this buckle.

The different character of the two types of motion is well illustrated in Figs. 20 and 21. In the large amplitude type of Fig. 20 the traveling wave type of motion is quite evident. The low amplitude motion of Fig. 21 is of the standing wave type. The two mode approximation clearly shows these differences. Both Figs. 22 and 23 show that the ratio of maximum amplitudes, $\theta_{1MAX}/\theta_{2MAX}$ is not far from 1. The phase shift, φ , is quite evident in the two cases. For the large amplitude flutter of Fig. 22 $\varphi \doteq 100^{\circ}$. While for the low amplitude flutter of Fig. 23 it is essentially zero. Comparison of the calculated points with the sine curves of Figs. 22, 23, and 24 show that the motion is essentially sinusoidal. A further check of the motion shows that the assumption used in Section H, Part II, that A_1, A_2, φ_1 and φ_2 are slowly varying functions of time is substantiated.

The assumptions of Ref. 10 and Part II are in the main substantiated. A study based upon use of additional modes is probably warranted.

The results of many of the tests are presented in Table II.

REFERENCES

1. Shen, S. F., Flutter of a Two-Dimensional Simply-supported Uniform Panel in a Supersonic Stream, Contract No. N5ori-07833, Office of Naval Research, Dept. Aero. Eng., M.I.T. August 6, 1952.

2. Miles, J. W., Dynamic Chordwise Stability at Supersonic Speeds, Rept. No. AL-1140, North American Aviation, Inc., October 18, 1950.

3. Goland, M. and Luke, Y. L., An Exact Solution for Two-Dimensional Linear Panel Flutter at Supersonic Speeds, Journal of the Aeronautical Sciences, Volume 21, 275, April 1954.

4. Nelson, H. C. and Cunningham, H. J., Theoretical Investigation of Flutter of Two-Dimensional Flat Panels with One Surface Exposed to Supersonic Potential Flow, NACA Technical Note 3465, July 1955.

5. Hedgepeth, J. M., Budiansky, B., and Leonard, R. W., Analysis of Flutter in Compressible Flow of a Panel on Many Supports, Journal of the Aeronautical Sciences, Volume 21, 475-486, July 1954.

6. Isaacs, R. P., Transtability Flutter of Supersonic Aircraft Panels, Rand Report P-101, July 1, 1949.

7. Hayes, W., A Buckled Plate in a Supersonic Stream, Rept. AL-1029, North American Aviation, Inc., May 10, 1950.

8. Miles, J. W., Dynamic Chordwise Stability at Supersonic Speeds, Rept. AL-1140. North American Aviation, Inc., Oct. 18, 1950.

9. Fung, Y. C., The Static Stability of a Two-Dimensional Curved Panel in a Supersonic Flow, with an Application to Panel Flutter. Journal of the Aeronautical Sciences, Vol. 21, 556-565, August 1954.

10. Fung, Y. C., The Flutter of a Buckled Plate in a Supersonic Flow, OSR-TN-55-237, July 1955.

11. Iguchi, S., Eine Lösung für die Berechnung der biegsamen rechteckigen Platten. Julius Springer, Berlin, 1933.

12. Wittrick, W. H., Buckling of Oblique Plates with Clamped Edges under Uniform Compression, The Aeronautical Quarterly, Volume IV, February 1953.

13. Miles, J. W., The Aerodynamic Forces on an Oscillating Air Foil at Supersonic Speeds, Journal of the Aeronautical Sciences, Volume 14, 351-358, June 1947.

14. Garrick, I. E., and Rubinow, S. I., Flutter and Oscillating Air-Force Calculations for an Airfoil in a Two-Dimensional Supersonic Flow, NACA Rept. No. 846, 1947.

15. Garrick, I. E., and Rubinow, F. I., Theoretical Study of Air Forces on an Oscillating or Steady Thin Wing in a Supersonic Main Stream, NACA Rept. No. 872, 1946.

16. Schwarz, L., Untersuchung einiger mit den Zylinderfunctionen Nullter Ordnung verwandter Funktionen. Luftfahrtforschung, Bd. 20 Lfg. 12, 341-372, February 8, 1944.

17. Luke, Y. L., Tables of Coefficients for Compressible Flutter Calculations. Air Force Tech. Rept. 6200, WADC, 1950.

18. Timoshenko, S., Vibration Problems in Engineering, Second Edition, D. Van Nostrand Company, Inc., 1937.

19. Timoshenko, S., Theory of Elastic Stability, McGraw-Hill Book Company, Inc., 1936.

20. Temple, G., Chapter IX, Unsteady Motion, Modern Developments in Fluid Dynamics, High Speed Flow, edited by L. Howarth, Oxford University Press, 1953.

APPENDIX A

Quasi-steady Theory

1) Aerodynamic Forces

$$\text{Let} \quad \Phi(x,y,z,t) = \Phi_1(x,y,z)\, e^{-i(\omega t - \Omega x)} \tag{1}$$

and substitute it into equation A-1, Part I. The reduced potential, $\Phi_1(x,y,z)$ then satisfies the equation

$$\beta^2 \frac{\partial^2 \Phi_1}{\partial x^2} - \frac{\partial^2 \Phi_1}{\partial y^2} - \frac{\partial^2 \Phi_1}{\partial z^2} + \frac{k^2 M^2}{\pi^2 \beta^2} \Phi_1 = 0 \tag{2}$$

The quasi-steady solution is formulated as follows (Ref. 20): Expand Φ_1 in a power series in terms of the reduced frequency, , and neglect all terms of order higher than the first. That is

$$\Phi_1 = \Phi_a + ik\Phi_b + O(k^2) + \cdots \tag{3}$$

The result of substituting equation 3 into 2 is

$$\beta^2 \frac{\partial^2 \Phi_a}{\partial x^2} - \frac{\partial^2 \Phi_a}{\partial y^2} - \frac{\partial^2 \Phi_a}{\partial z^2} = 0$$

and (4)

$$\beta^2 \frac{\partial^2 \Phi_b}{\partial x^2} - \frac{\partial \Phi_b}{\partial y^2} - \frac{\partial^2 \Phi_b}{\partial z^2} = 0$$

The boundary conditions are developed as follows:

$$\left(\frac{\partial \Phi_1}{\partial y}\right)_{y=0} = \left(\frac{\partial \Phi_a}{\partial y}\right)_{y=0} + ik\left(\frac{\partial \Phi_b}{\partial y}\right)_{y=0}$$

$$= \left\{ U \frac{\partial Y_1}{\partial x}(x,z) - \frac{ikU}{\pi} Y_1(x,z) \right\} e^{-i\Omega x} \tag{5}$$

where

$$\bar{y} = Y_1(x,z)\, e^{-i\omega t} \tag{6}$$

and $\bar{y}$ is the plate deflection.

Equating real and imaginary parts

$$\left(\frac{\partial \varphi_a}{\partial y}\right)_{y=0} = U e^{-i\Omega x} \frac{\partial y_1}{\partial x}(x,z)$$

$$\left(\frac{\partial \varphi_b}{\partial y}\right)_{y=0} = -\frac{U}{\pi} e^{-i\Omega x} y_1(x,z) \tag{7}$$

Equations 4 are of the form of the well known potential equation for steady flow. The solution to this equation is

$$\varphi(x,y,z) = -\frac{1}{\pi}\int_0^{\xi_1} d\xi \int_{\eta_1}^{\eta_2} \frac{\left(\frac{\partial \varphi}{\partial y}\right) d\eta}{\sqrt{(x-\xi)^2 - \beta^2\left[(z-\eta)^2 + y^2\right]}} \tag{8}$$

where

$$\xi_1 = x - \beta y$$

$$\eta_1 = z - \sqrt{\frac{(x-\xi)^2}{\beta^2} - y^2}$$

$$\eta_2 = z + \sqrt{\frac{(x-\xi)^2}{\beta^2} - y^2}$$

If the boundary condition is applied at the surface equation 8 becomes

$$\varphi(x,+0,z) = -\frac{1}{\pi}\int_0^{\xi_1} d\xi \int_{\eta_1}^{\eta_2} \frac{\left(\frac{\partial \varphi}{\partial y}\right)_{y=0} d\eta}{\sqrt{(x-\xi)^2 - \beta^2(z-\eta)^2}} \tag{9}$$

where

$$\xi_1 = x$$

$$\eta_1 = z - \frac{(x-\xi)}{\beta}$$

$$\eta_2 = z + \frac{(x-\xi)}{\beta}$$

The above integral represents an integration over the forward Mach cone. The same difficulties are present when trying to perform this integration as were present in the exact solution. The discussion on pages 10 and 11 holds here as well. In the following the quasi-steady problem is worked out in detail according to the method described on those pages.

Equation 9 can be simplified by the following substitution

$$\eta = \eta_0 \cos\theta + z \qquad \eta_0 = \frac{(x-\xi)}{\beta} \tag{10}$$

If the specific boundary conditions of equation 5 are employed there results

$$\varphi_a = -\frac{U}{\pi\beta}\int_0^x e^{-i\Omega\xi} d\xi \int_0^\pi \frac{\partial Y_1}{\partial \xi}\left(\xi, \eta[\theta]\right) d\theta$$

$$\varphi_b = \frac{U}{\pi^2\beta}\int_0^x e^{-i\Omega\xi} d\xi \int_0^\pi Y_1\left(\xi, \eta[\theta]\right) d\theta \tag{11}$$

Assume a deflection of the form

$$Y_1 = A_{mm} \sin\frac{m\pi x}{L_1} \sin\frac{m\pi z}{L_2} \tag{12}$$

Then

$$I_a = \int_0^{\pi} \frac{\partial \gamma_1}{\partial \xi}\, d\theta$$

$$= A_{mm}\, m \cos m\xi \left\{ \cos \frac{m\pi z}{L_2} \int_0^{\pi} \sin\left(\frac{m\pi \eta_0}{L_2} \cos\theta\right) d\theta \right.$$

$$\left. + \sin \frac{m\pi z}{L_2} \int_0^{\pi} \cos\left(\frac{m\pi \eta_0}{L_2} \cos\theta\right) d\theta \right\} \qquad (13)$$

$$I_b = \int_0^{\pi} \gamma_1\, d\theta$$

$$= A_{mm} \sin m\xi \left\{ \cos \frac{m\pi z}{L_2} \int_0^{\pi} \sin\left(\frac{m\pi \eta_0}{L_2} \cos\theta\right) d\theta \right.$$

$$\left. + \sin \frac{m\pi z}{L_2} \int_0^{\pi} \cos\left(\frac{m\pi \eta_0}{L_2} \cos\theta\right) \right.$$

But

$$\int_0^{\pi} \sin\left(\frac{m\pi \eta_0}{L_2} \cos\theta\right) d\theta = 0$$

$$\int_0^{\pi} \cos\left(\frac{m\pi \eta_0}{L_2} \cos\theta\right) d\theta = \pi J_0\left(\frac{m\pi \eta_0}{L_2}\right) \qquad (14)$$

Thus

$$I_a = A_{mm} \cos m\xi \left(\sin \frac{m\pi z}{L_2}\right) \pi J_0\left(\frac{m\pi \eta_0}{L_2}\right)$$

$$I_b = A_{mm} \sin m\xi \left(\sin \frac{m\pi z}{L_2}\right) \pi J_0\left(\frac{m\pi \eta_0}{L_2}\right) \qquad (15)$$

Equation 11 become

$$\varphi_a = -A_{mm}\frac{Um}{\beta}\sin\frac{m\pi z}{L_2}\int_0^x e^{-i\Omega\xi}\cos m\xi\, J_0(\lambda\varkappa)\,d\xi$$

$$\varphi_b = A_m\frac{U}{\beta\pi}\sin\frac{m\pi z}{L_2}\int_0^x e^{-i\Omega\xi}\sin m\xi\, J_0(\lambda\varkappa)\,d\xi \qquad (16)$$

where

$$\lambda = \frac{m\pi}{L_2\beta} \qquad \varkappa = (x-\xi)$$

Equations 16 can be put into a more useful form

$$\varphi_a = -A_{mm}\frac{Um}{2\beta}\sin\frac{m\pi z}{L_2}\left\{\int_0^x e^{-i(\Omega-m)\xi}J_0(\lambda\varkappa)\,d\xi + \int_0^x e^{-i(\Omega+m)\xi}J_0(\lambda\varkappa)\,d\xi\right.$$

$$\varphi_b = A_{mm}\frac{iU}{2\beta\pi}\sin\frac{m\pi z}{L_2}\left\{-\int_0^x e^{-i(\Omega-m)\xi}J_0(\lambda\varkappa)\,d\xi + \int_0^x e^{-i(\Omega+m)\xi}J_0(\lambda\varkappa)\,d\xi\right. \qquad (17)$$

The integrals in the above equations are of the same form as equation A-7, Part I. They can be reduced to the Schwarz function notation. The following integrals are defined

$$\varphi_c = \int_0^x e^{-i(\Omega+m)\xi}J_0(\lambda\varkappa)\,d\xi$$

$$= x\,e^{-i(\Omega+m)x}\,\bar{f}_0\left[\frac{\Omega+m}{\lambda},(\Omega+m)x\right] \qquad (18)$$

$$\varphi_D = \int_0^x e^{-i(\Omega - m)\xi} J_0(\lambda \bar{x}) d\xi$$

$$= x e^{-i(\Omega-m)x} \bar{f}_0 \left[\frac{\Omega - m}{\lambda}, (\Omega + m)x \right] \qquad (18 \text{ cont'd})$$

Equations 17 are now

$$\varphi_a = -\frac{U}{2\beta} A_{mn} m \sin \frac{m\pi z}{L_2} (\varphi_c + \varphi_D)$$

$$\varphi_b = \frac{iU}{2\pi\beta} A_{mn} \sin \frac{m\pi z}{L_2} (\varphi_c - \varphi_D) \qquad (19)$$

The complete potential is then

$$\varphi = \varphi_1 e^{-i(\omega t - \Omega x)} = (\varphi_a + ik\varphi_b) e^{-i(\omega t - \Omega x)}$$

$$= -A_{mn} \frac{U}{2\beta\pi} \sin \frac{m\pi z}{L_2} \left\{ (m\pi + k)\varphi_c + (m\pi - k)\varphi_D \right\} e^{-i(\omega t - \Omega x)} \qquad (20)$$

The pressure is

$$p_{mn} = A_{mn} \frac{\rho U^2}{2\beta\pi} \sin \frac{m\pi z}{L_2} \left\{ 2m\pi J_0(\lambda x) \right.$$

$$\left. -(m^2\pi + 2km) i \varphi_c + (m^2\pi - 2km) i \varphi_D \right\} e^{-i(\omega t - \Omega x)} \qquad (21)$$

Equation 21 is the pressure distribution due to a deflection of the form of equation 12.

If a deflection of the form of equation A-15, Part I is assumed, it follows in a similar manner that

$$\Phi_a = -A_{mm}\frac{U_m}{\beta}\int_0^x e^{-i\Omega\xi}\cos m\xi \left\{A_0 + \sum_{r=1}^{\infty} A_r \cos\frac{2r\pi z}{L_2}\; J_0(\gamma R)\, d\xi\right.$$

$$= -\frac{U}{\beta}A_{mm}\left\{A_0 B + \frac{1}{2}\sum_{r=1}^{\infty} A_r \cos\frac{2r\pi z}{L_2}\left(\Phi_E + \Phi_F\right)\right.$$

$$\Phi_b = A_{mm}\frac{U}{\beta\pi}\int_0^x e^{-i\Omega\xi}\sin m\xi \left\{A_0 + \sum_{r=1}^{\infty} A_r \cos\frac{2r\pi z}{L_2}\; J_0(\gamma R)\, d\xi\right\} \qquad (22)$$

$$= A_{mm}\frac{U}{\beta\pi}\left\{A_0 D + \frac{i}{2}\sum_{r=1}^{\infty} A_r \cos\frac{2r\pi z}{L_2}\left(\Phi_E - \Phi_F\right)\right\}$$

where

$$B = \int_0^x e^{-i\Omega\xi}\cos m\xi\, d\xi$$

$$D = \int_0^x e^{-i\Omega\xi}\sin m\xi\, d\xi \qquad (23)$$

$$\Phi_E = \int_0^x e^{-i(\Omega+m)\xi}\, J_0(\gamma R)\, d\xi$$

$$= x\, e^{-i(\Omega+m)x}\, \bar{f}_0\left[\frac{\Omega+m}{\gamma}, (\Omega+m)x\right]$$

$$Q_F = \int_0^x e^{-i(\Omega-m)\xi} J_0(\gamma R)\, d\xi$$

$$= x\, e^{-i(\Omega-m)x}\, \bar{f}_0\left[\frac{\Omega-m}{\gamma}, (\Omega-m)x\right] \tag{24}$$

and $\gamma = \frac{2r\pi}{L_2\beta}$

If terms of order k^2 are neglected

$$B = \frac{1}{m^2}\left\{e^{-i\Omega x}\left[-i\Omega\cos mx + m\sin mx\right] + i\Omega\right\}$$

$$D = \frac{1}{m^2}\left\{e^{-i\Omega x}\left[-i\Omega\sin mx - m\cos mx\right] + m\right\} \tag{25}$$

The complete potential is

$$\Phi = -A_{mm}\frac{U}{2\beta\pi}\left\{2(m\pi B - ikD)A_0\right.$$

$$+ (m\pi + k)\left[\sum_{r=1}^{\infty} A_r\left(\cos\frac{2r\pi z}{L_2}\right) Q_E\right]$$

$$\left.+ (m\pi - k)\left[\sum_{r=1}^{\infty} A_r\left(\cos\frac{2r\pi z}{L_2}\right) Q_F\right]\right\} e^{-i(\omega t - \Omega x)} \tag{26}$$

The pressure relation is

$$p_{mm} = A_{mm}\frac{\rho a U^2}{2\beta\pi}\left\{2m\pi\sum_{r=1}^{\infty} A_r\cos\frac{2r\pi z}{L_2}\, J_0(\gamma x)\right.$$

$$\left.- (m^2\pi + 2mk)\, i\sum_{r=1}^{\infty} A_r\cos\frac{2r\pi z}{L_2}\, Q_E\right. \tag{27}$$

$$+(m^2\pi - 2mk)\, i \sum_{r=1}^{\infty} A_r \cos \frac{2r\pi z}{L_2} \quad Q_F$$

$$+ 2A_0 e^{-i\Omega x}\left[(\Omega\pi - 2k)\sin mx + m\pi \cos mx\right]\Big\} e^{-i(\omega t - \Omega x)}$$

To find the pressure on a finite plate as shown in Fig. 1 the above pressure relation equation 2-40 is added to equation 2-34 and this sum is then divided by two. The result is

$$(p_{mn})_{\text{FINITE PLATE}} = A_{mn} \frac{\rho_a U^2}{4\beta\pi} e^{-i(\omega t - \Omega x)}\Big\{2m\pi\left[J_0(\lambda x)\sin\frac{n\pi z}{L_2} + \sum_{r=1}^{\infty} A_r \cos\frac{2r\pi z}{L_2} J_0(\gamma x)\right] - (m^2\pi + 2mk)\left[i Q_C \sin\frac{n\pi z}{L_2} + i\sum_{r=1}^{\infty} A_r \cos\frac{2r\pi z}{L_2} Q_E\right] + (m^2\pi - 2mk)\left[i Q_D \sin\frac{n\pi z}{L_2} + i\sum_{r=1}^{\infty} A_r \cos\frac{2r\pi z}{L_2} Q_F\right] + 2A_0 e^{-i\Omega x}\left[m\pi\cos mx + (\Omega\pi - 2k)\sin mx\right]\Big\} \tag{28}$$

The generalized forces obtained from substituting equation 28 into equation B-13, Part I, are

for $m \neq l$

$$Q_{mls} = \frac{\rho_a U^2}{2\beta\pi} \frac{i m l}{(m^2 - l^2)}\Big\{(m\pi + 2k)\left[I_{02}(m) + \sum_{r=1}^{\infty} A_r^2 I_{08}(m)\right] \tag{29}$$

$$-(m\pi - 2k)\left[I_{o\lambda}(-m) + \sum_{r=1}^{\infty} A_r^2\, I_{o\gamma}(-m)\right]$$

$$+(l\pi + 2k)\left[I_{o\lambda}(l) + \sum_{r=1}^{\infty} A_r^2\, I_{o\gamma}(l)\right]$$

$$-(l\pi - 2k)\left[I_{o\lambda}(-l) + \sum_{r=1}^{\infty} A_r^2\, I_{o\gamma}(-l)\right]\Bigg\}$$

(29 cont'd)

$$+\frac{2\rho_a U^2}{s\beta\pi} A_o m^2 \left\{1-(-1)^s\right\}\left\{1-(-1)^{m+l}\right\}$$

for $m = l$

$$Q_{mls} = \frac{\rho_a U^2 m}{4\beta}\Bigg\{i\left[I_{o\lambda}(m) + \sum_{r=1}^{\infty} A_r^2\, I_{o\gamma}(m)\right]$$

$$-i\left[I_{o\lambda}(-m) + \sum_{r=1}^{\infty} A_r^2\, I_{o\gamma}(-m)\right]$$

$$+(m\pi + 2k)\left[I_{o\lambda}(m) + \sum_{r=1}^{\infty} A_r^2\, I_{o\gamma}(m)\right.$$

$$\left.-I_{1\lambda}(m) - \sum_{r=1}^{\infty} A_r^2\, I_{1\gamma}(m)\right]$$

$$+(m\pi-2k)\left[I_{o\lambda}(-m)+\sum_{r=1}^{\infty}A_r^2\,I_{o\delta}(-m)\right. \tag{30}$$

$$\left.-I_{1\lambda}(-m)-\sum_{r=1}^{\infty}A_r^2\,I_{1\delta}(m)\right]\Big\}$$

$$+\frac{\rho_a U^2}{2S\pi\beta}A_o\left\{1-(-1)^s\right\}\left\{\Omega\pi-2k\right\}$$

These values of Q_{mmls} may be used to solve the determinant equation C-1, Part I. In this case the Q_{mmls}'s depend upon the AR ratio; therefore each case must be carried out separately.

TABLE I

M = 2.18 γ = 60

A_2	φ	A_1	Q	λ_1	k
0.5	180	2.95	1.26	2.59	0
	170	3.53	1.45	2.64	0.200
	160	4.67	1.78	2.76	0.340
	150	5.56	1.98	2.87	0.418
0.8	180	3.2	2.3	2.81	0
	175	3.8	2.7	2.86	0.161
	170	4.9	3.2	2.98	0.238
	160	6.9	4.3	3.25	0.366
	150	8.5	4.8	3.53	0.449
1.0	180	3.3	3.3	2.97	0
	175	4.4	3.9	3.1	0.184
	170	5.9	4.9	3.28	0.274
	165	7.3	5.8	3.48	0.335
	160	8.5	6.5	3.66	0.377

TABLE II

Trace No.	h	λ^*_{1B}	λ^*_{1A}	Q_{CR}	γ	κ	ξ	Type
129	0.031	9.5		2.75	60.7			
132		8.8		3.10	54.4			
134		13.7		2.63	64.1			
139		13.5		2.65	63.8			
140		14.3		2.60	65.0			
142		11.4		2.74	61.8			
144		9.8		2.94	57.8			
145		14.9		2.54	66.8			
161		11.1	10.6	2.75	64.6**	0.242	73	
162		4.2	3.5	2.94		0.414	125	L. A.***
163		9.9	9.4	2.94		0.242	73	
165		3.3	4.1	3.13		0.414	125	L. A.
166		3.1	4.0	3.10		0.421	127	L. A.
168		3.2	3.8	3.26		0.428	129	L. A.
169		3.4	4.0	2.92		0.414	125	L. A.
170		4.2	4.6	2.89		0.408	123	L. A.
173		10.4	10.0	2.75		0.236	71	
175		12.4	11.9	2.68		0.202	61	
177		5.8	5.0	2.58				L. A.
178		13.3	12.9	2.66		0.186	56	
180		6.1	5.3	2.78				L. A.
181		10.7	10.2	2.78		0.246	74	
183	↓	12.4	12.1	2.68	62.18	0.196	60	
199	0.032	12.4	12.0	2.23		0.085	26	
200	↓	10.0	9.5	2.42		0.082	25	

TRACE NO.	h	λ_{1B}	λ_{1A}	Q_{CR}	γ	k	f	TYPE
201		10.9	10.4	2.41	65.1	0.085	26	
203		6.5	5.7	2.56				L. A.
204		8.3	7.7	2.56		0.088	27	
205		8.7	8.0	2.55		0.085	25	
206		7.4	6.7	2.71				
207		8.1	7.5	2.70		0.108	33	
209		5.9	5.3	2.79		0.062	19	
210		7.7	7.0	2.79		0.052	16	
211		6.7	6.0	2.96		0.056	17	
212		6.6	5.9	2.94				L. A.
213		5.5	4.8	3.07				
214		5.4	4.7	3.07				
216		5.0	4.3	3.21				
217		6.1	5.4	3.03				
218		8.1	7.4	2.62		0.091	28	
219		11.6	11.1	2.34		0.091	28	
220		11.9	11.4	2.24	70.1	0.085	26	
250	0.031		2.1	2.47	68.4			L. A.
251				2.47				L. A.
252			1.27	2.61				L. A.
267				2.61	59.8	0.460	140	L. A.
275		11.8	12.7	2.77		0.214	65	
276				2.93				L. A.
278			3.4	2.93				L. A.
279		2.3	5.0	2.93		0.362	110	L. A.

TRACE No	h	λ_{1_B}	λ_{1_A}	Q_{cr}	γ	K	f	TYPE
280	↓	4.5	6.3	2.93		0.388	118	L.A.
283		8.6	9.6	2.92		0.220	67	
284		2.3	5.0	2.72	61.1			L.A.
285		3.4		2.72				L.A.
288		12.2	13.1	2.72		0.181	55	
289		11.6	12.4	2.72		0.220	67	
291		11.3	12.2	2.77	60.2	0.191	58	

*Subscript B refers to calibration before test run; subscript A refers to calibration after test run.

**From Trace 161 on the temperature varied over a narrow range so records were not taken for every trace.

***Low Amplitude.

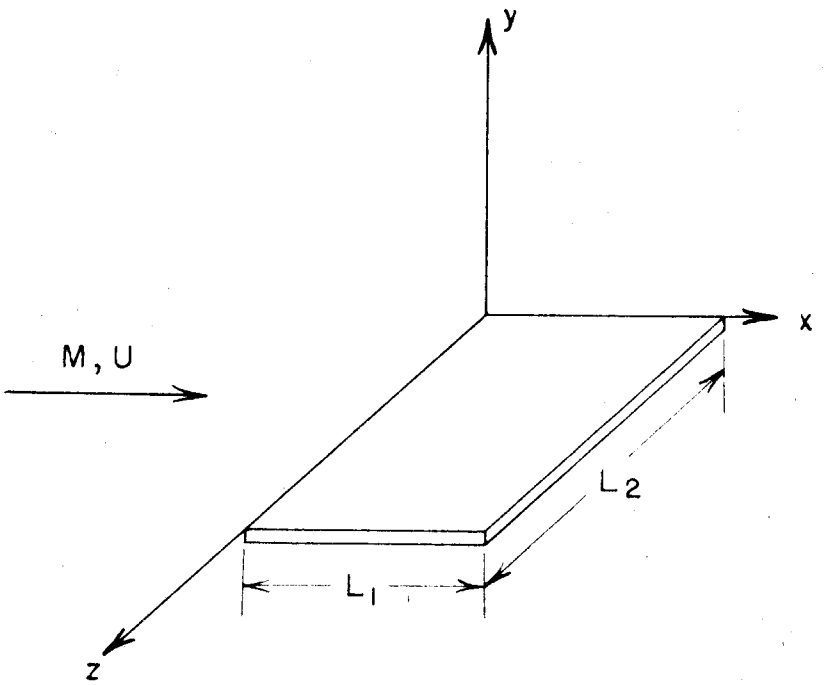

FIG. 1

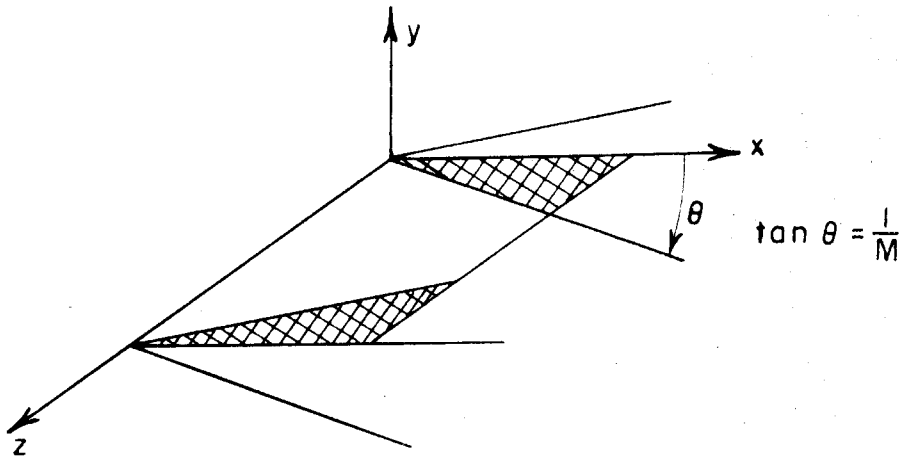

FIG. 2

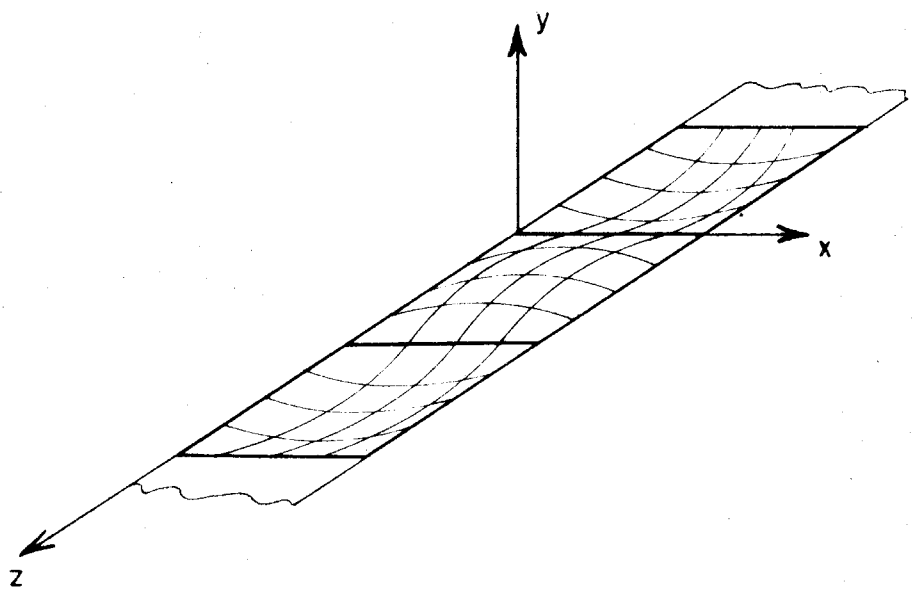

FIG. 3

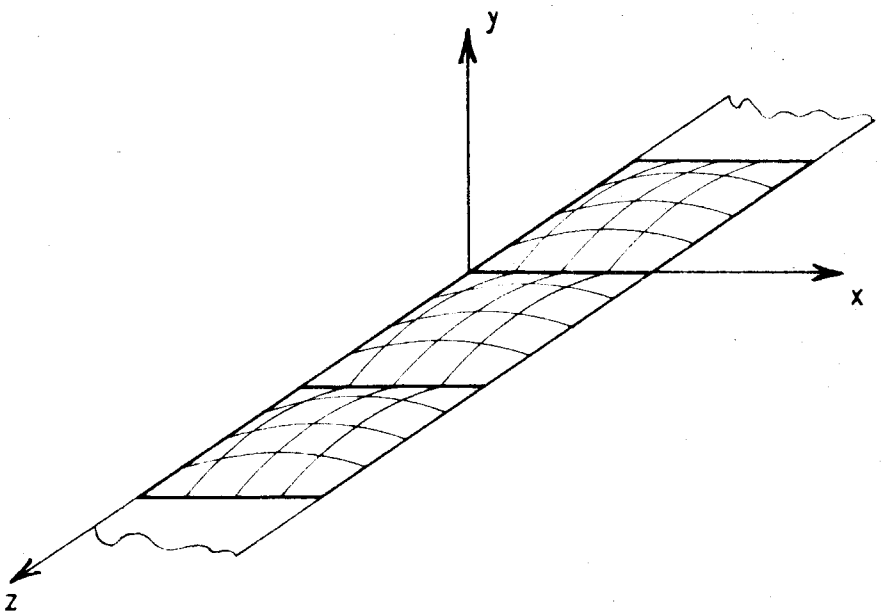

FIG. 4

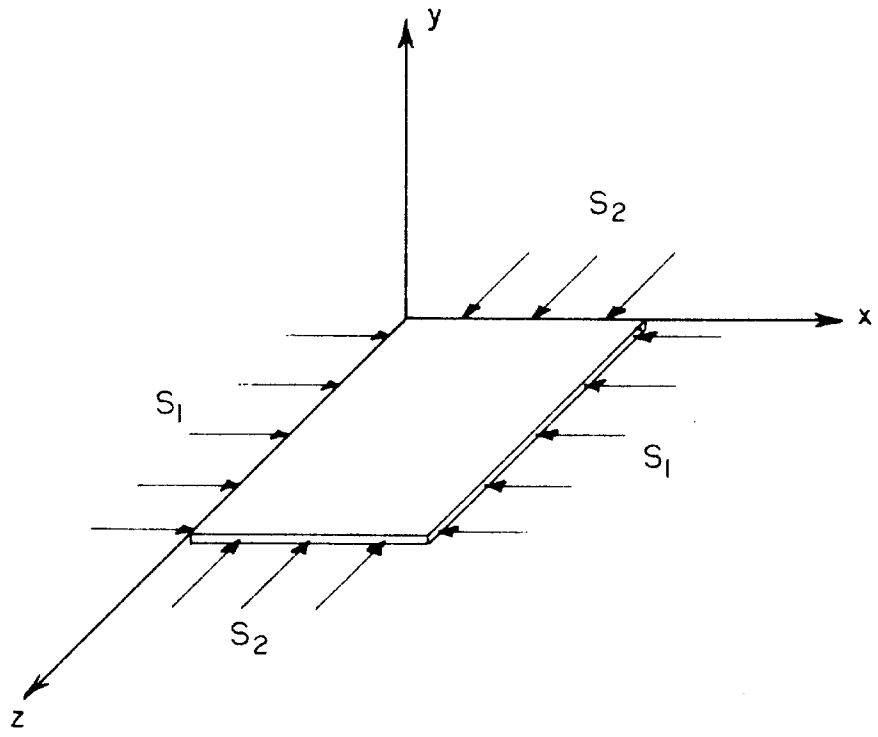

FIG. 5

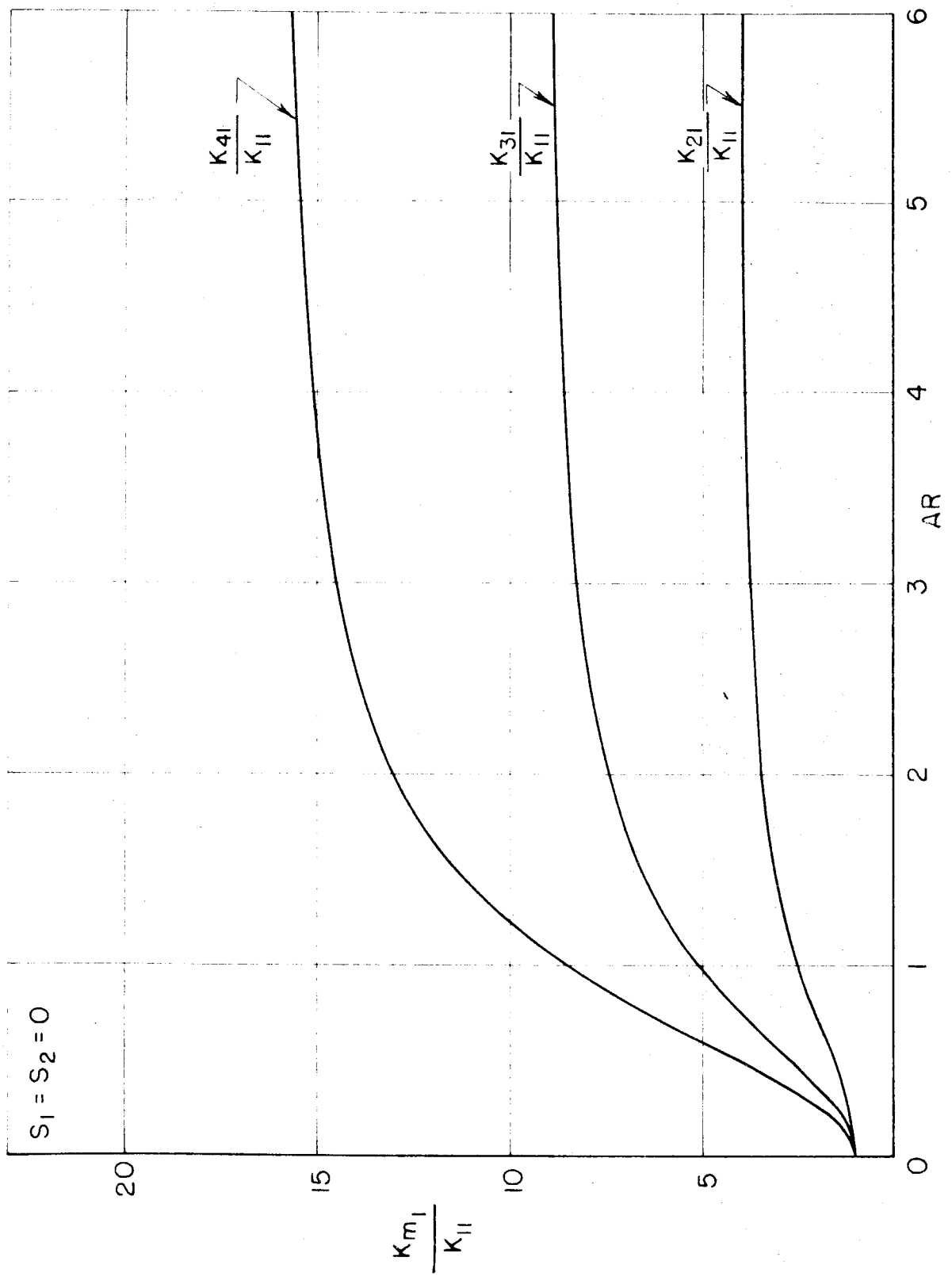
$S_1 = S_2 = 0$
$\frac{K_{m_1}}{K_{11}}$
20
15
10
5
0
1
2
3
AR
4
5
6
$\frac{K_{41}}{K_{11}}$
$\frac{K_{31}}{K_{11}}$
$\frac{K_{21}}{K_{11}}$

FIG. 6

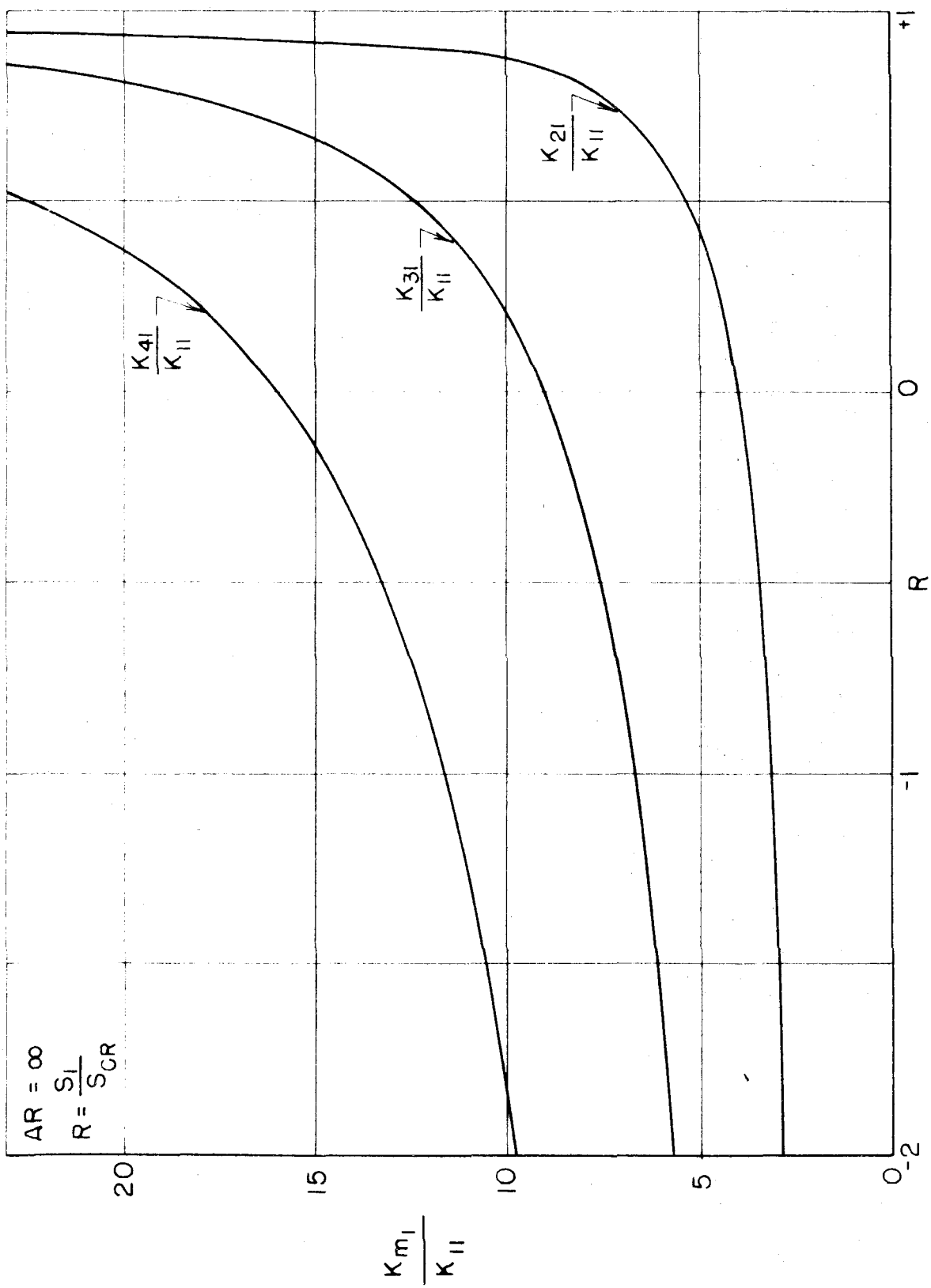

FIG. 7

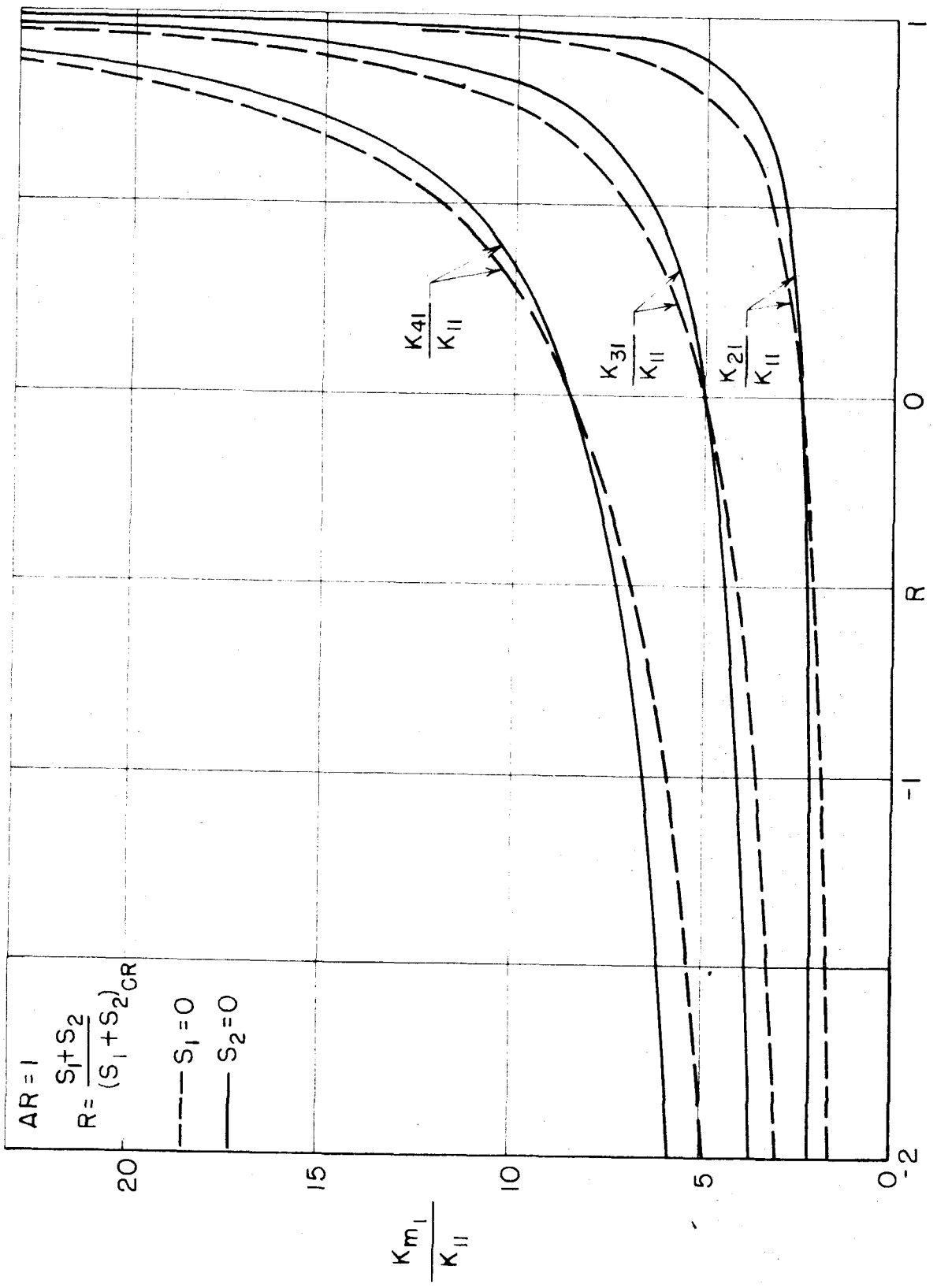
AR = 1
$R = \frac{S_1+S_2}{(S_1+S_2)_{CR}}$
$S_1 = 0$
$S_2 = 0$
$\frac{K_{m_1}}{K_{11}}$
$\frac{K_{41}}{K_{11}}$
$\frac{K_{31}}{K_{11}}$
$\frac{K_{21}}{K_{11}}$
20
15
10
5
0
-2
-1
0
1
R

FIG. 8

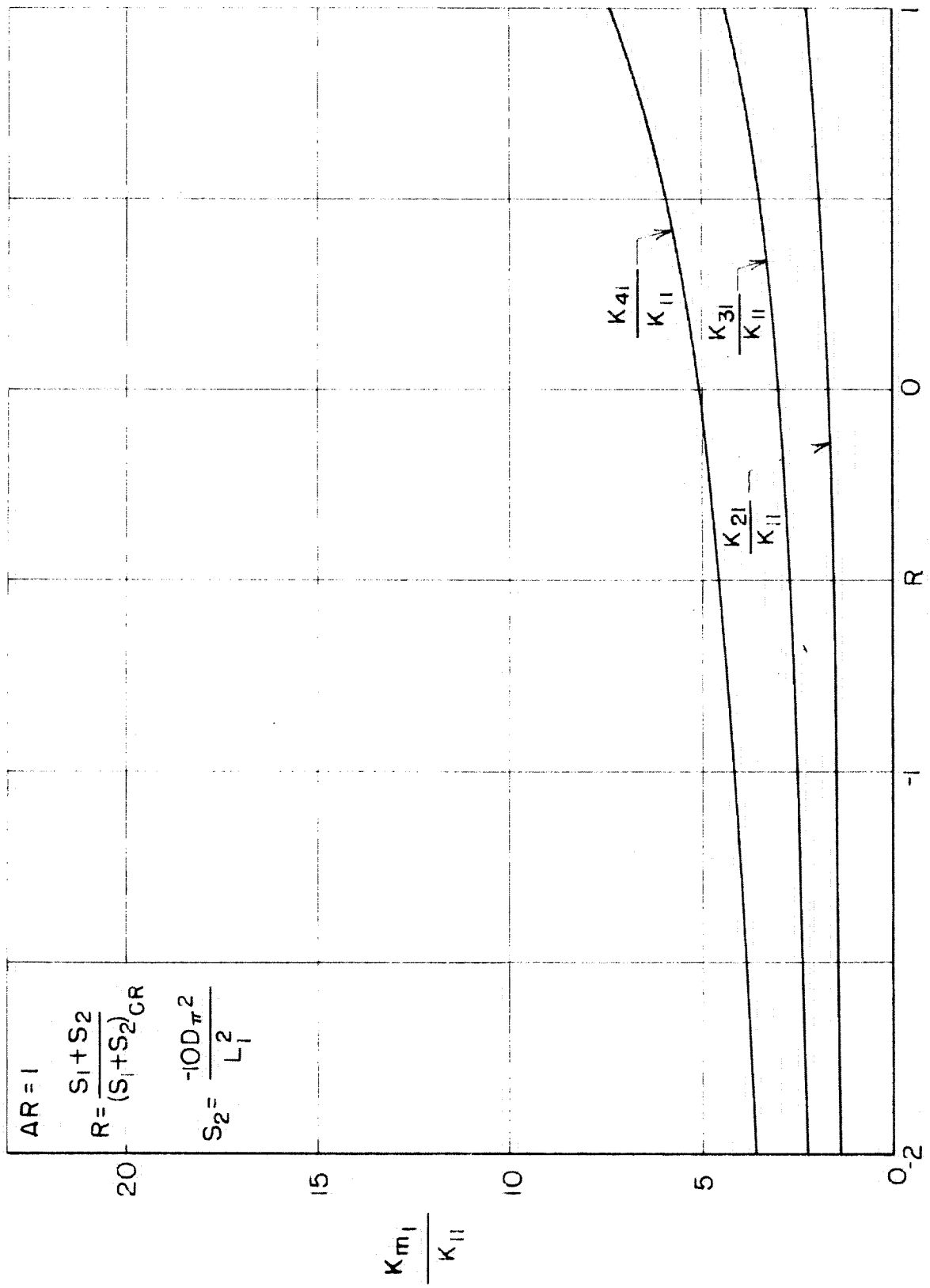
ΔR = 1
$R = \frac{S_1 + S_2}{(S_1 + S_2)_{CR}}$
$S_2 = \frac{-10 D_\pi^2}{L_1^2}$
$\frac{K_{m1}}{K_{11}}$
20
15
10
5
0
-2
-1
0
R
1
$\frac{K_{41}}{K_{11}}$
$\frac{K_{31}}{K_{11}}$
$\frac{K_{21}}{K_{11}}$

FIG. 9

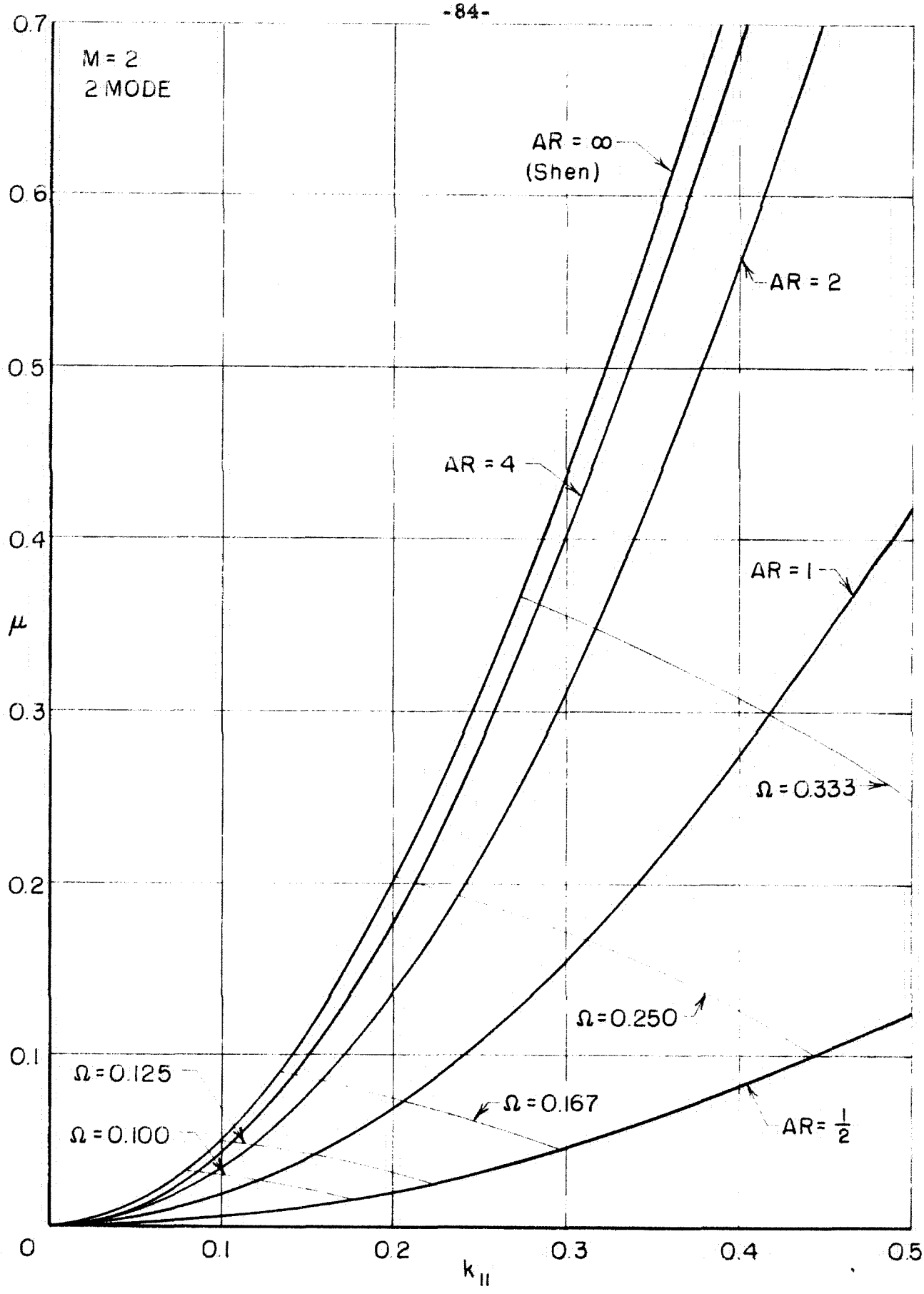
M = 2
2 MODE
AR = ∞
(Shen)
AR = 2
AR = 4
AR = 1
AR = ½
Ω = 0.333
Ω = 0.250
Ω = 0.167
Ω = 0.125
Ω = 0.100
μ
k_II
0
0.1
0.2
0.3
0.4
0.5
0.6
0.7

FIG. 10

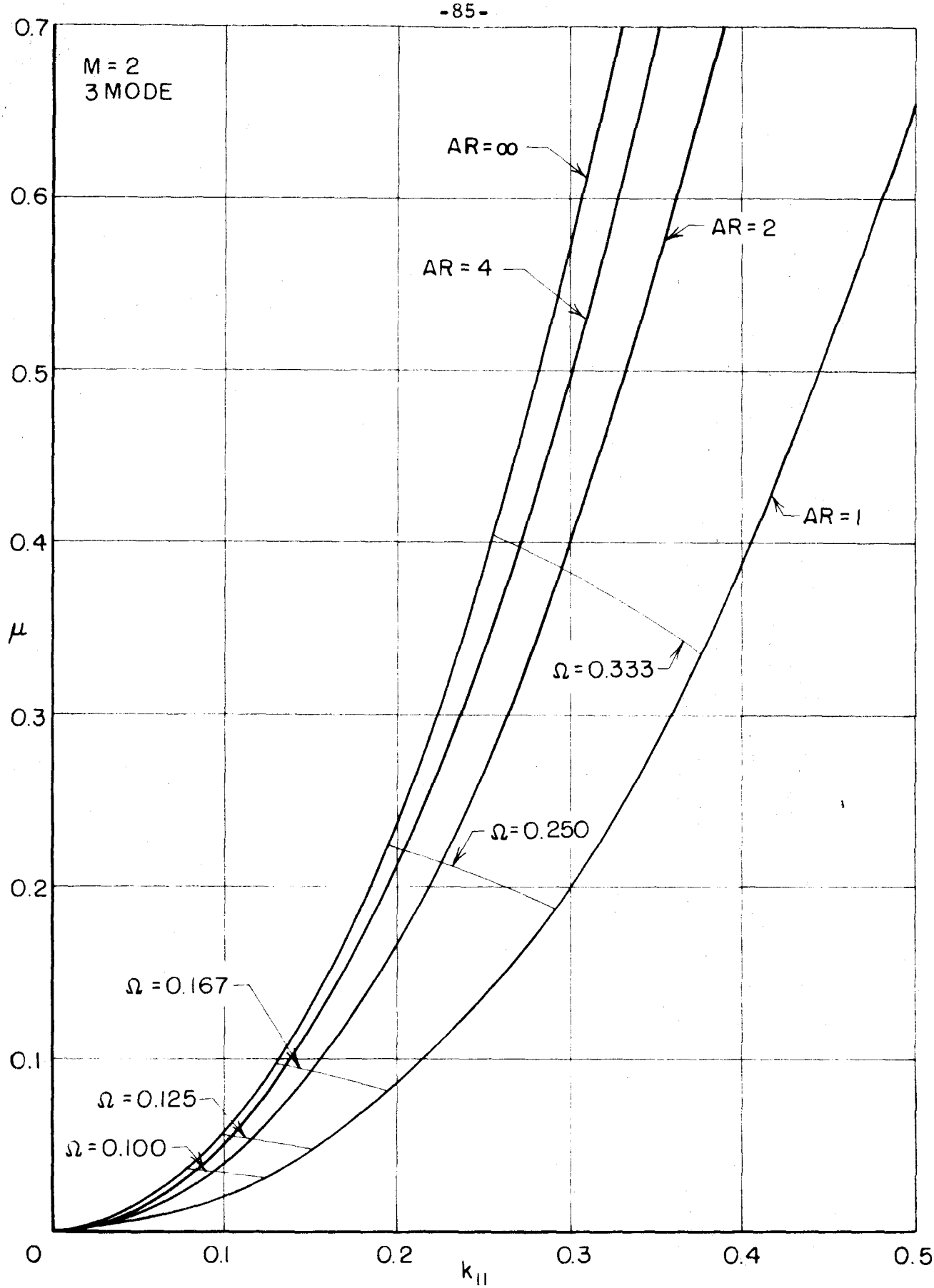
M = 2
3 MODE
AR = ∞
AR = 2
AR = 4
AR = 1
Ω = 0.333
Ω = 0.250
Ω = 0.167
Ω = 0.125
Ω = 0.100
μ
k11
0
0.1
0.2
0.3
0.4
0.5
0.6
0.7

FIG. 11

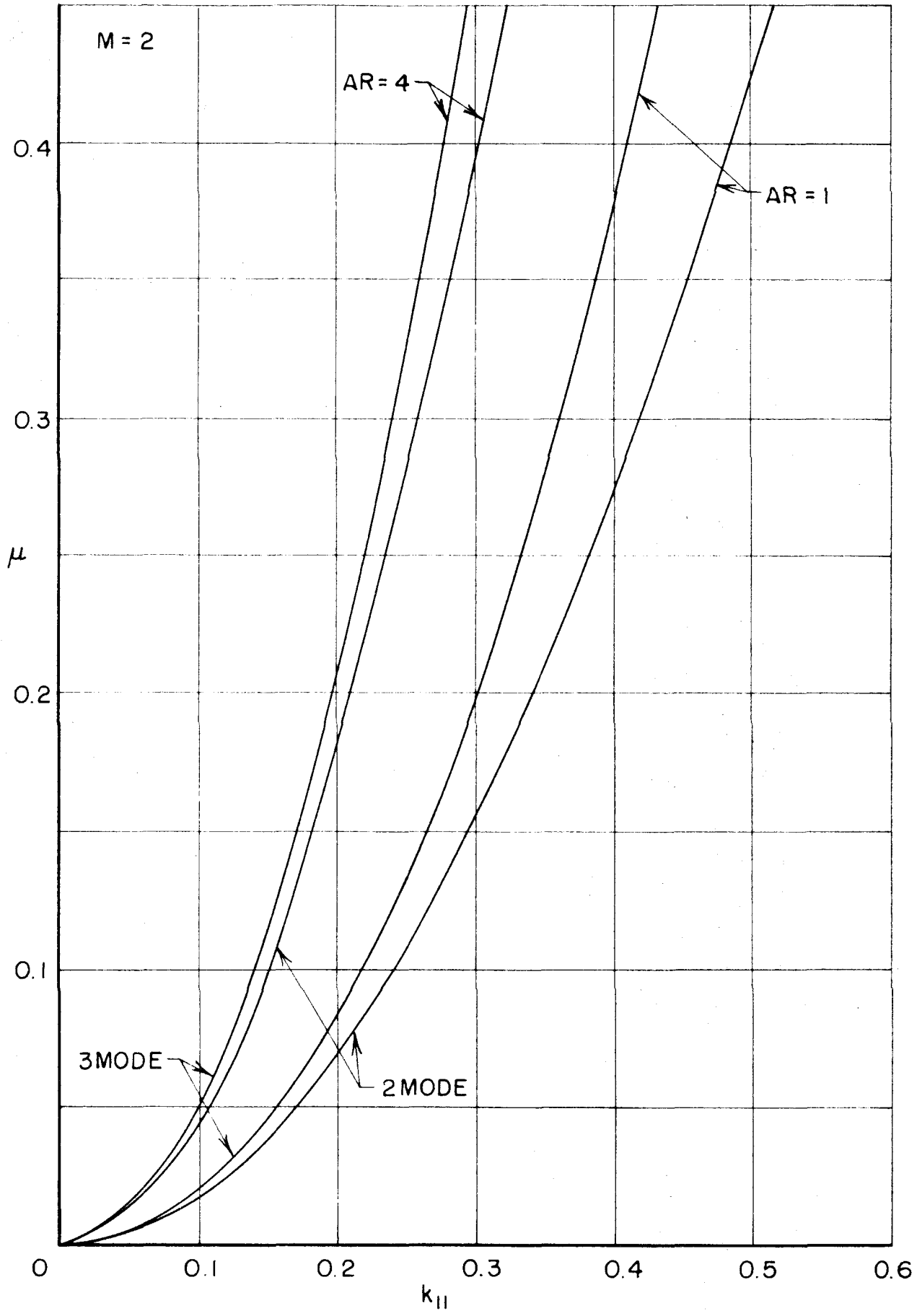

FIG. 12

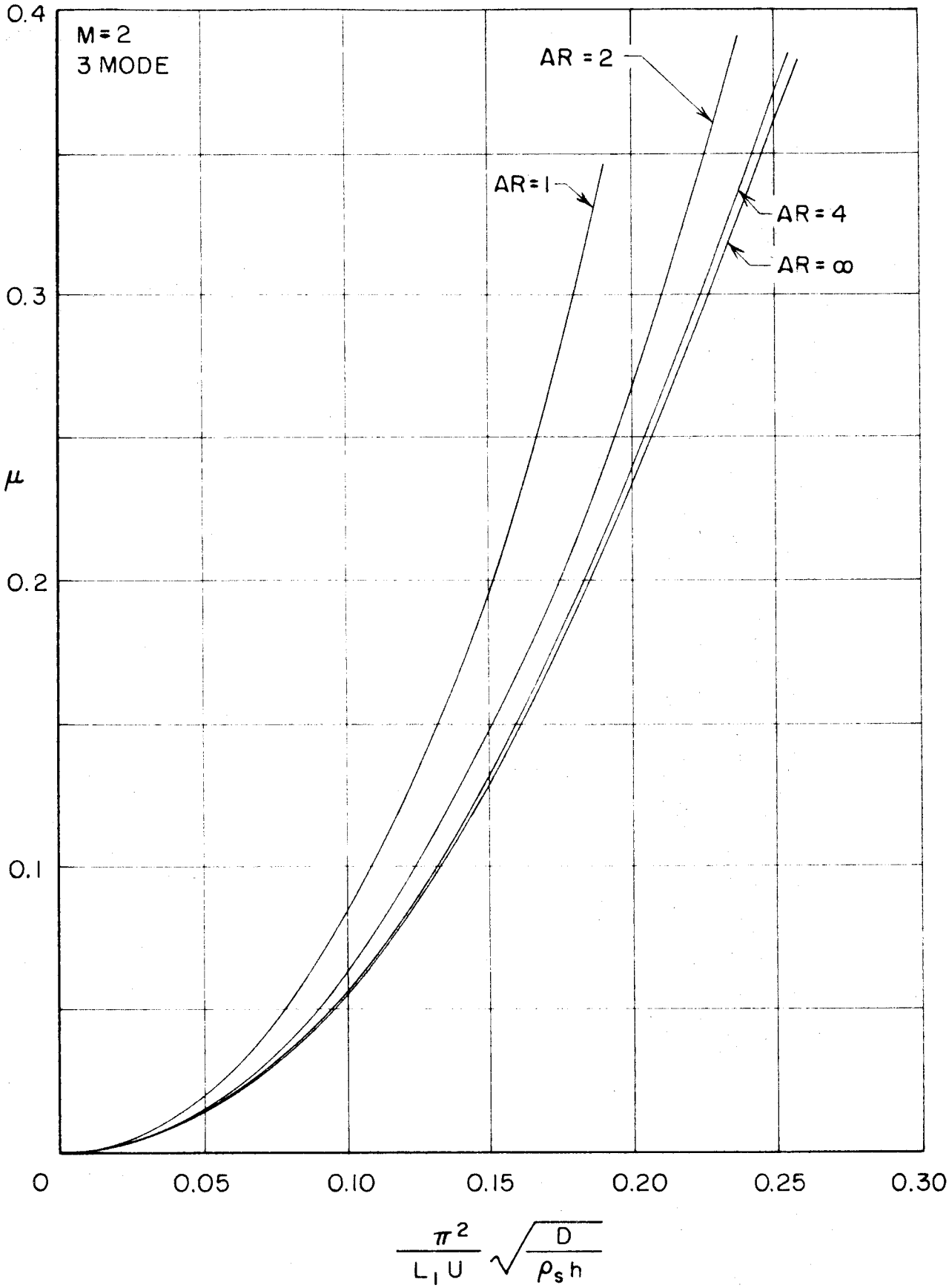
M = 2
3 MODE
AR = 2
AR = 1
AR = 4
AR = ∞
0.4
0.3
0.2
0.1
μ
0
0.05
0.10
0.15
0.20
0.25
0.30
$\frac{\pi^2}{L_1 U}\sqrt{\frac{D}{\rho_s h}}$

FIG. 13

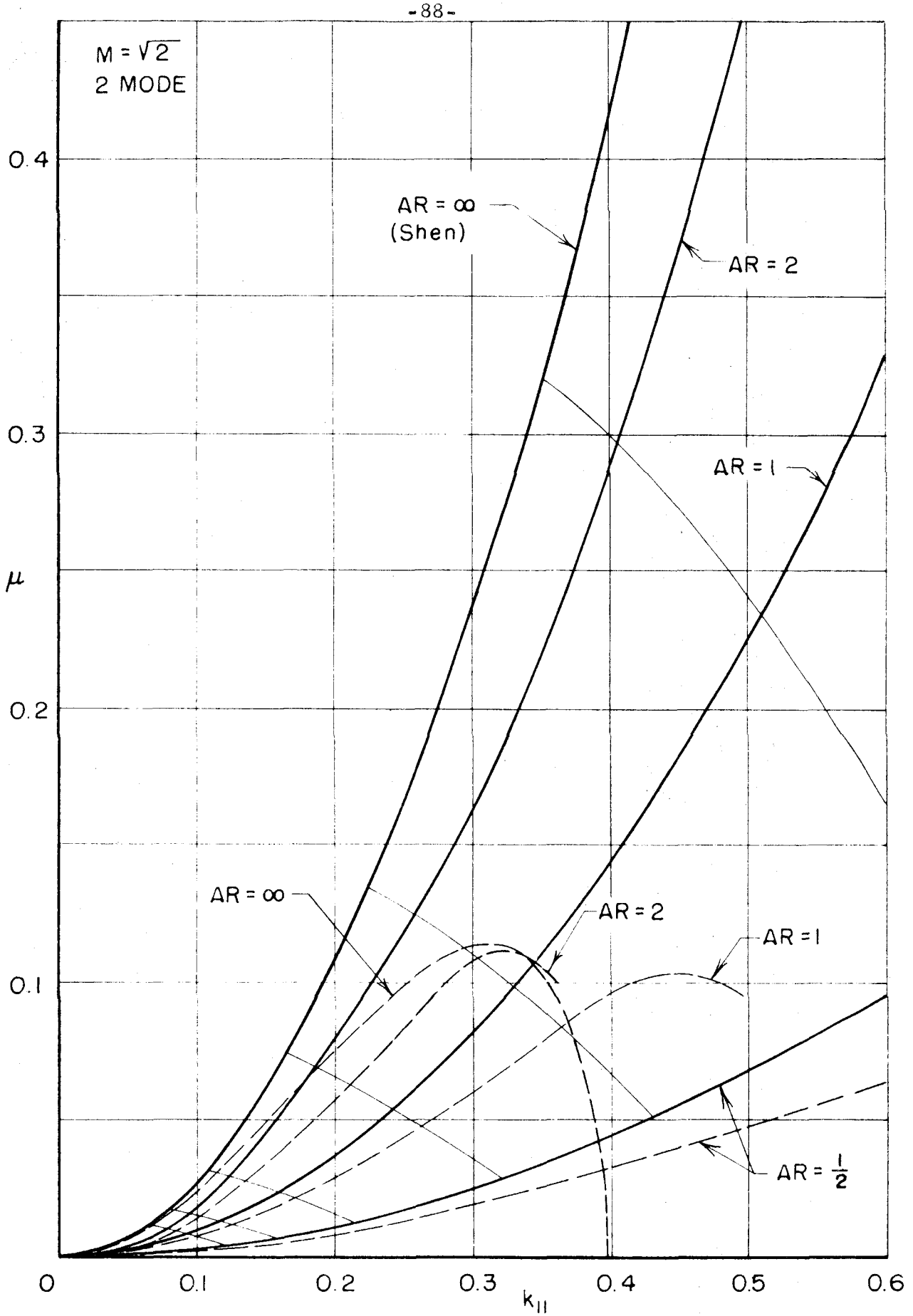
M = √2
2 MODE
AR = ∞
(Shen)
AR = 2
AR = 1
AR = ∞
AR = 2
AR = 1
AR = 1/2
μ
0.4
0.3
0.2
0.1
0
0.1
0.2
0.3
0.4
0.5
0.6
k11

FIG. 14

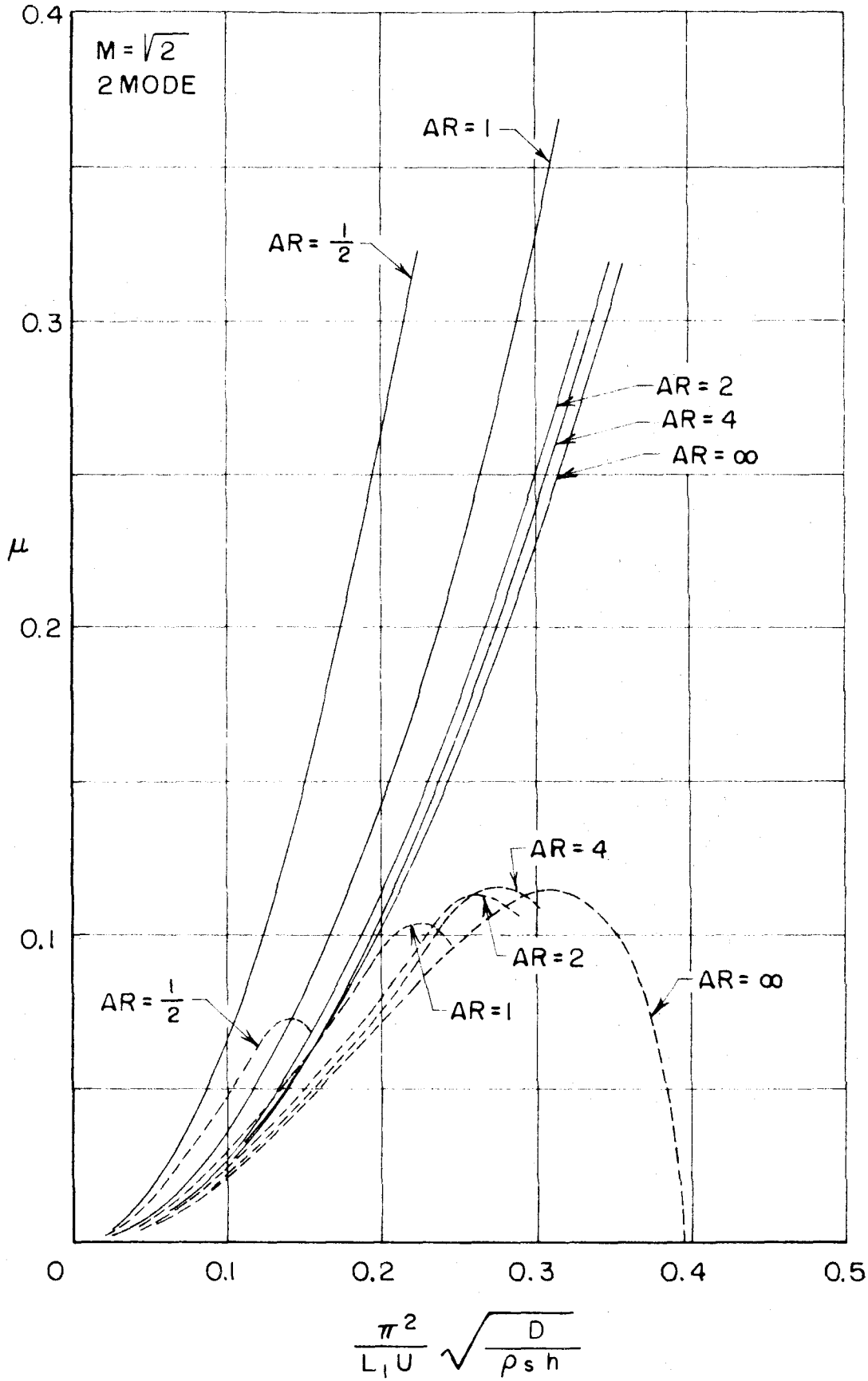
M = √2
2 MODE
AR = 1
AR = 1/2
AR = 2
AR = 4
AR = ∞
AR = 4
AR = 2
AR = ∞
AR = 1/2
AR = 1
μ
0.4
0.3
0.2
0.1
0
0.1
0.2
0.3
0.4
0.5
π² / L₁U √(D / ρs h)

FIG. 15

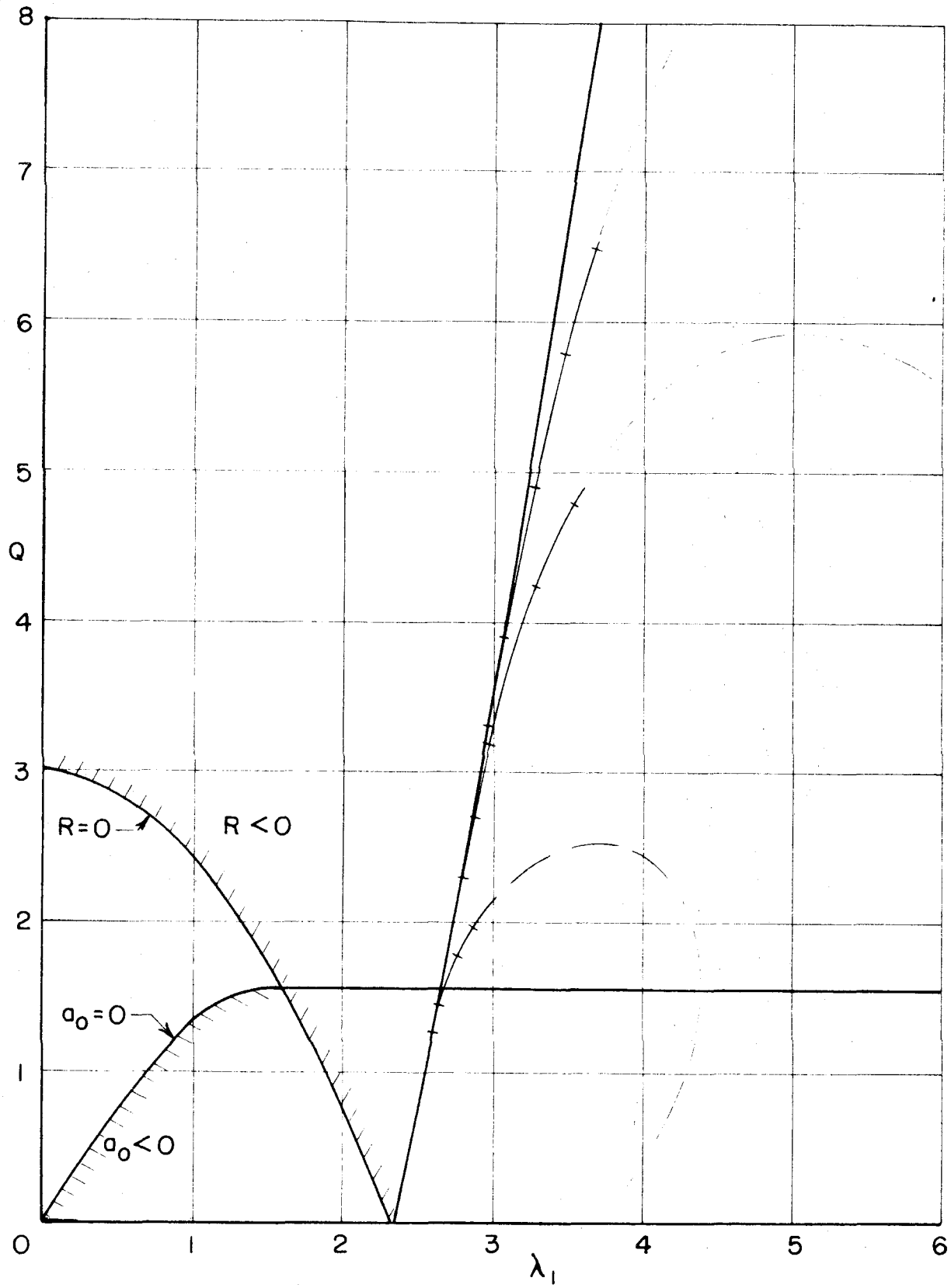

FIG. 16

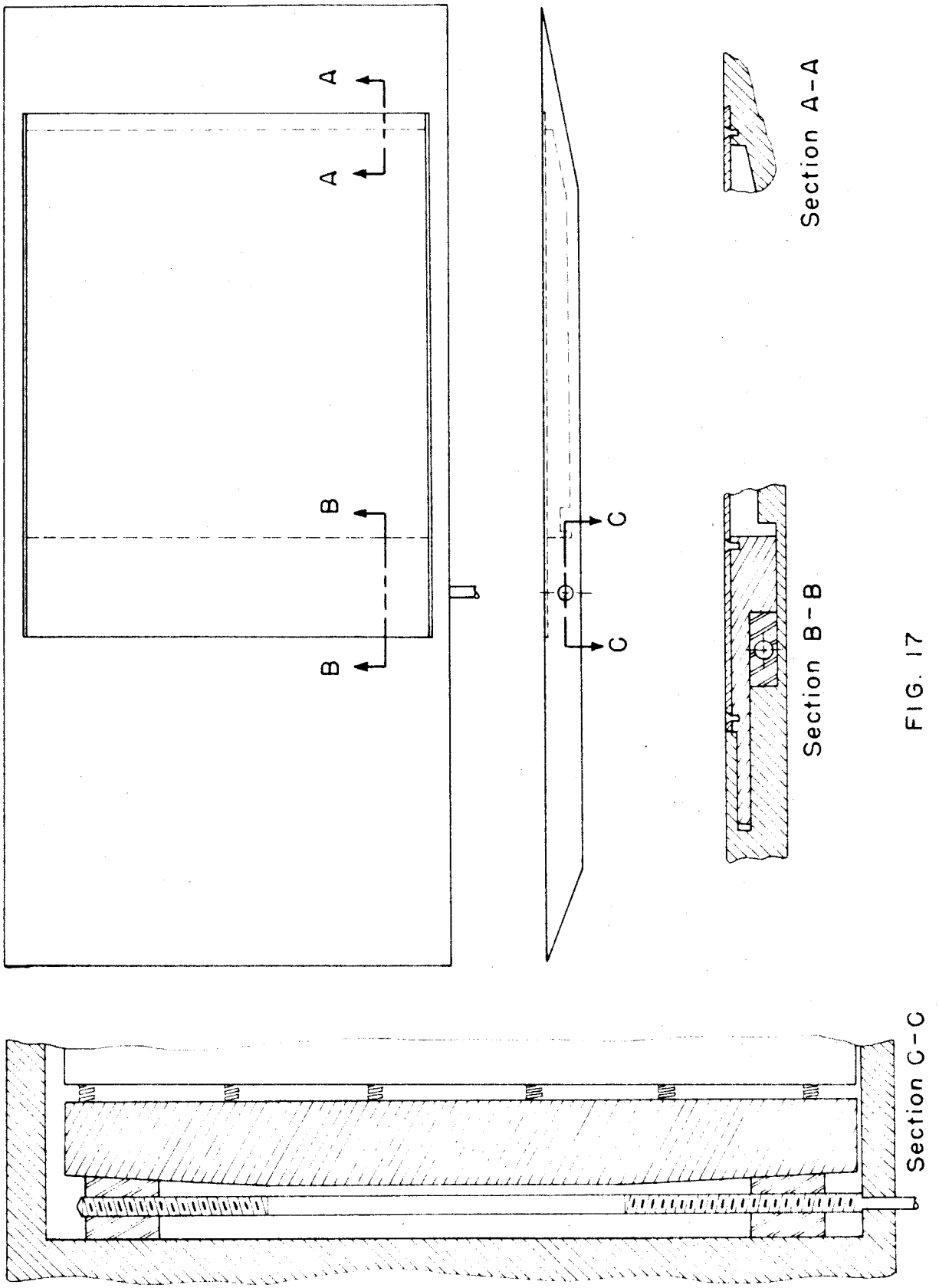

FIG. 17

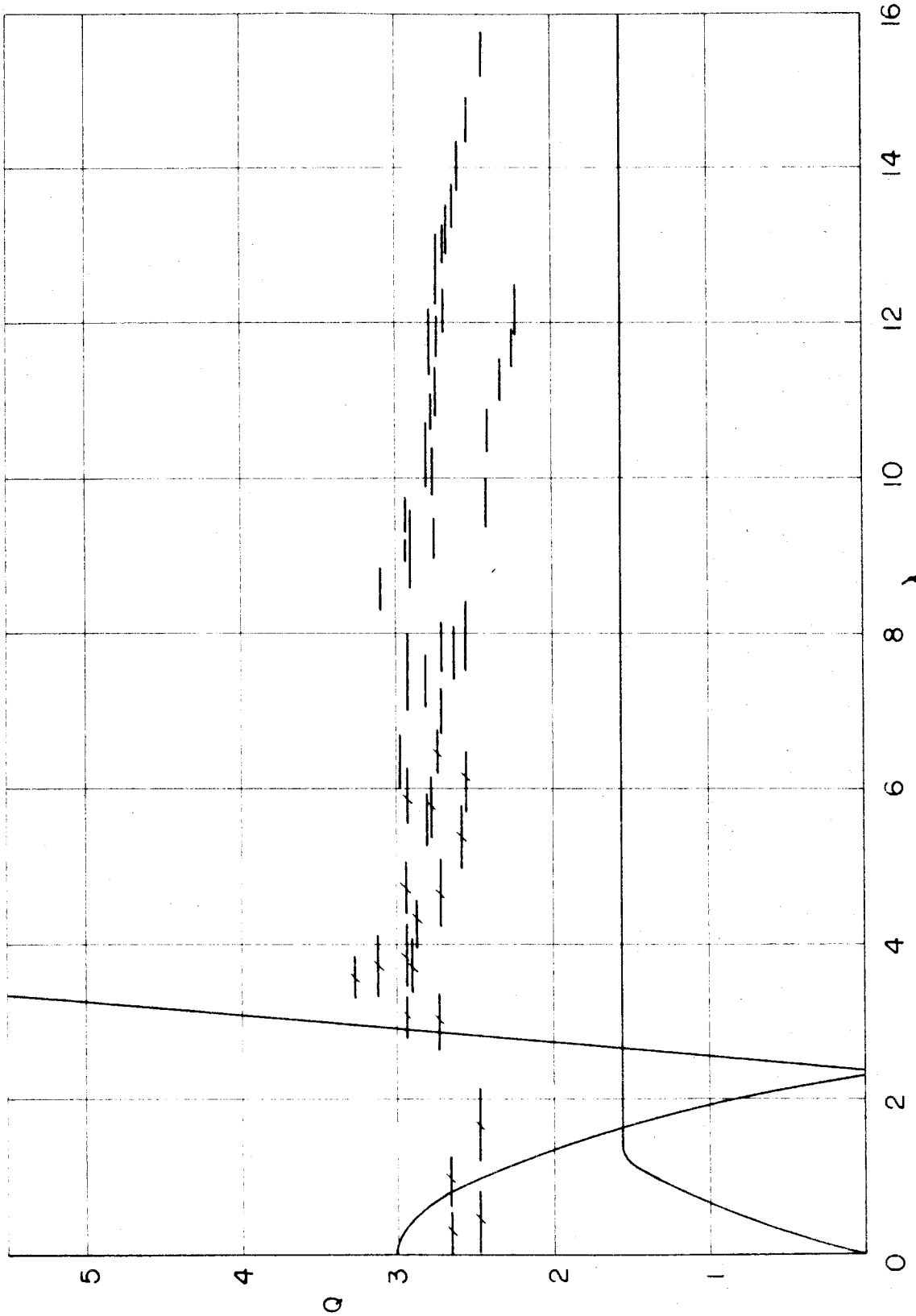

FIG. 18

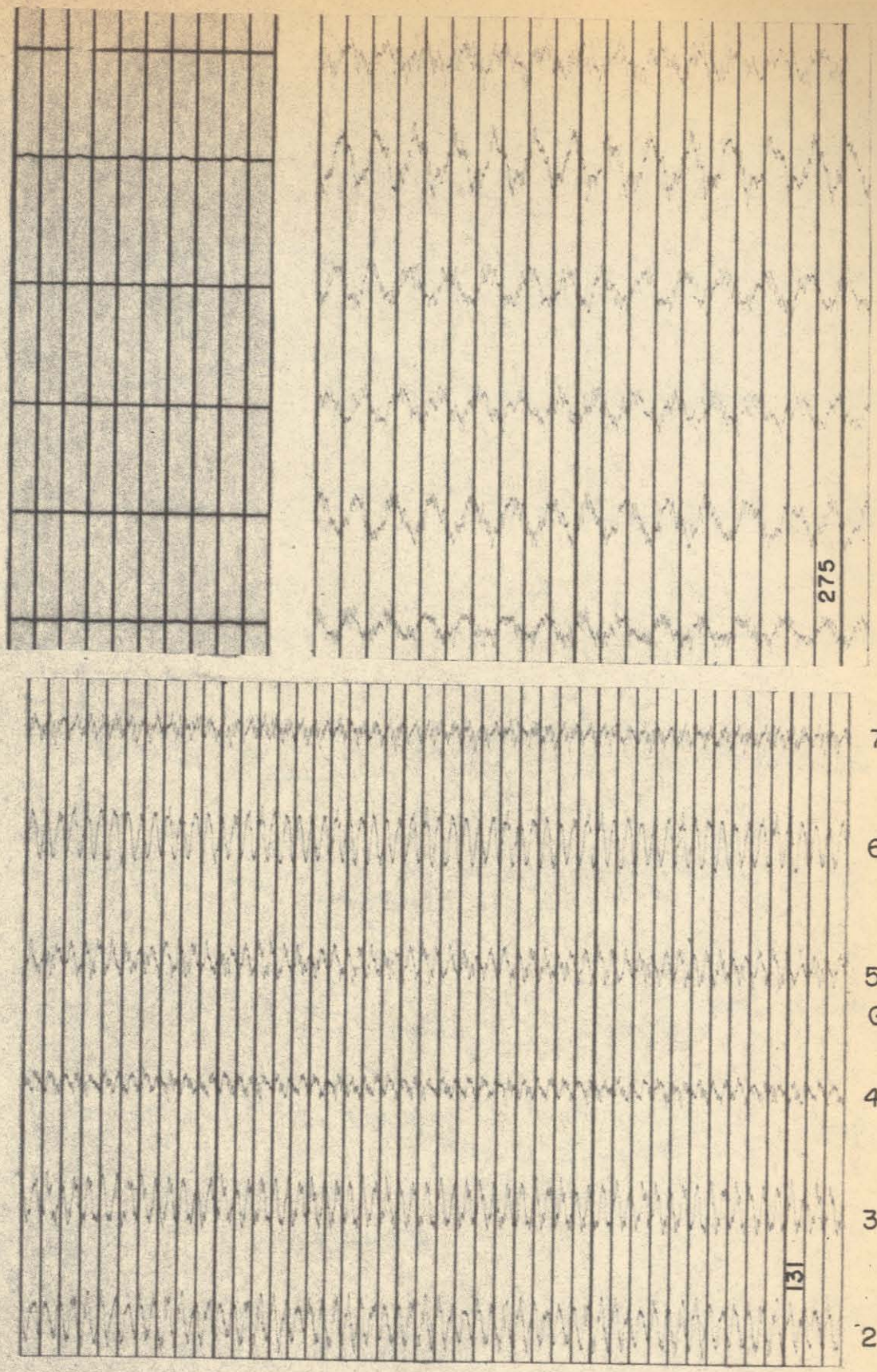

FIG. 19

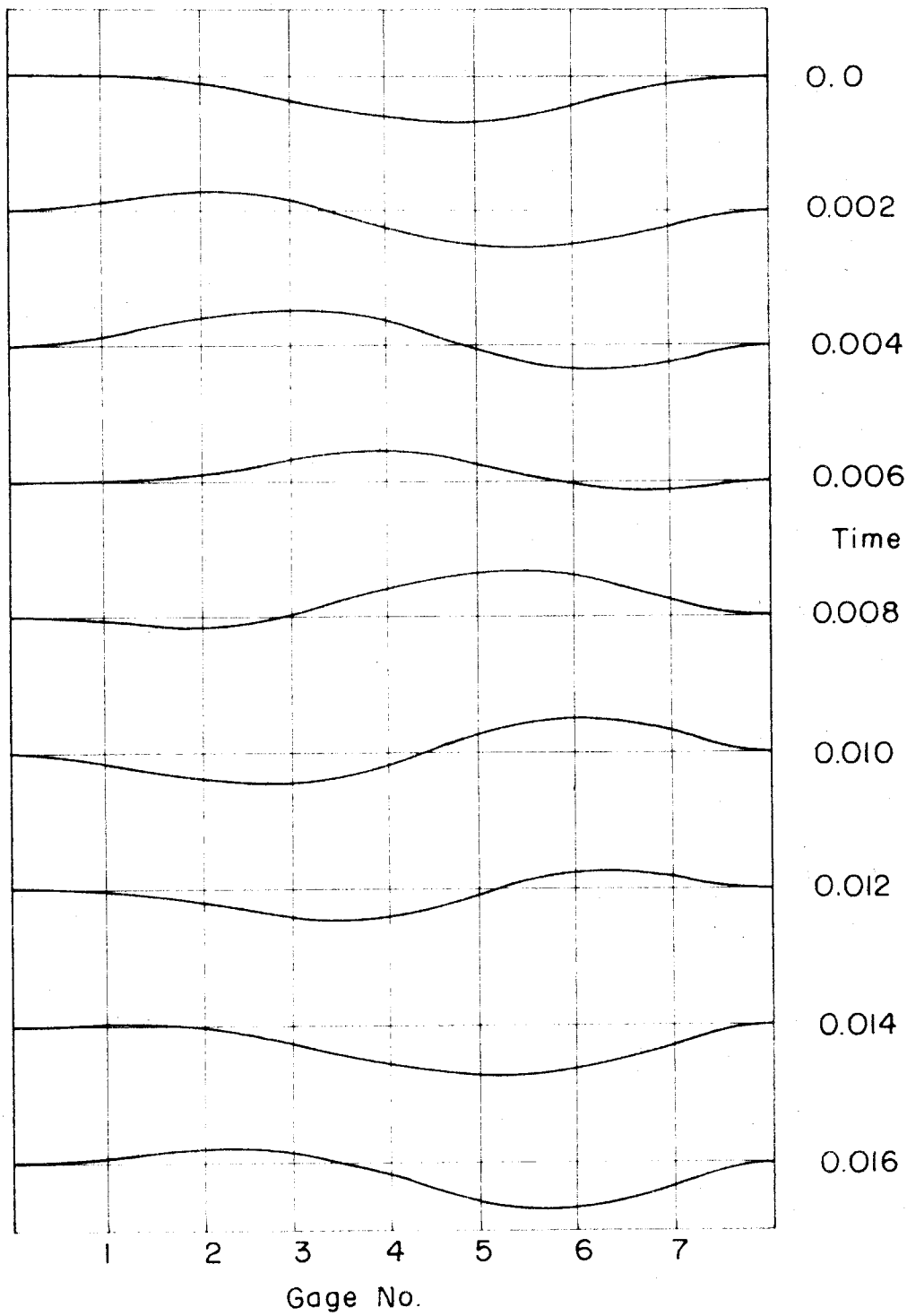
0.0
0.002
0.004
0.006
Time
0.008
0.010
0.012
0.014
0.016
1
2
3
4
5
6
7
Gage No.

FIG. 20

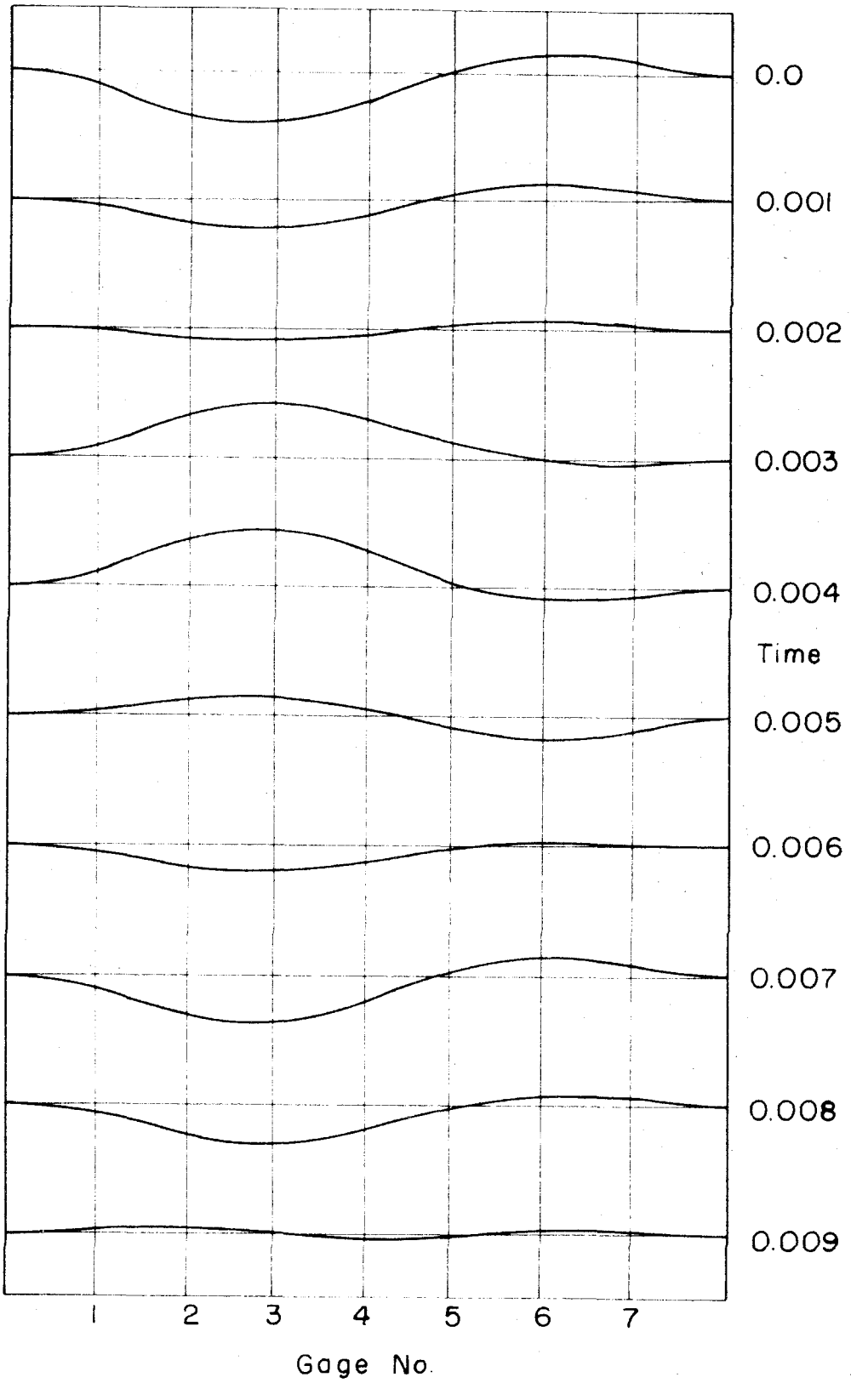
0.0
0.001
0.002
0.003
0.004
Time
0.005
0.006
0.007
0.008
0.009
1
2
3
4
5
6
7
Gage No.

FIG. 21

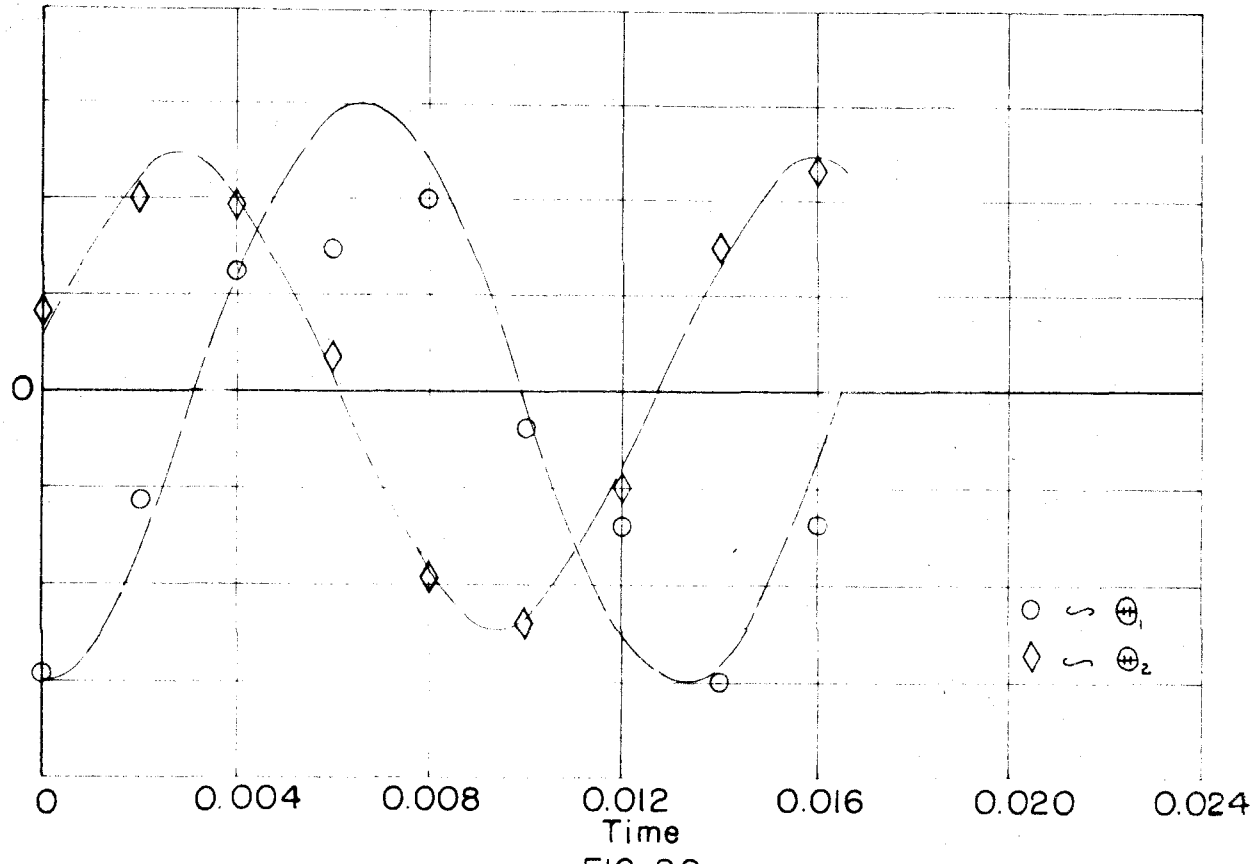
0
0
0.004
0.008
0.012
0.016
0.020
0.024
Time
Θ_1
Θ_2

FIG. 22

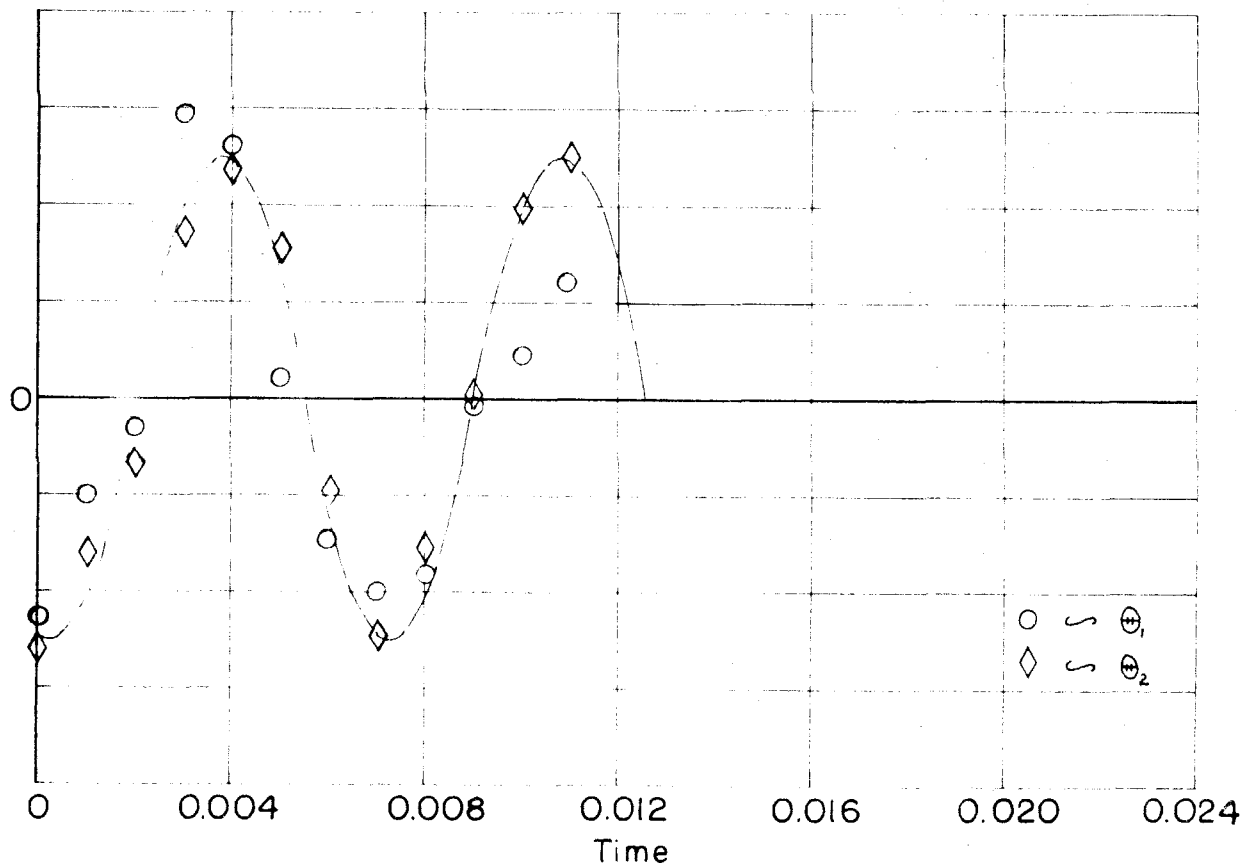
0
0
0.004
0.008
0.012
0.016
0.020
0.024
Time
Θ_1
Θ_2

FIG. 23

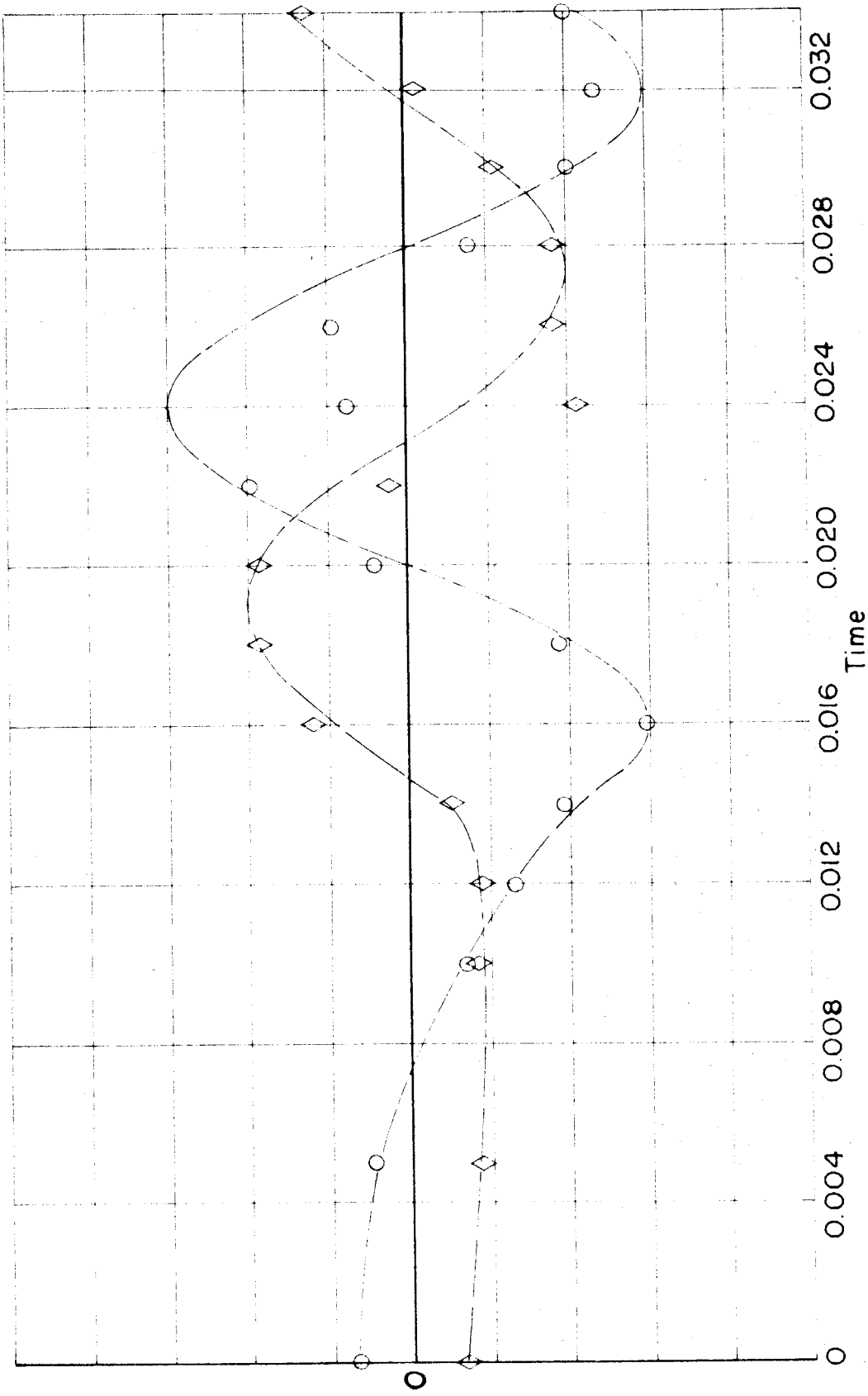

FIG. 24